

**Passivation Behavior of Copper Thin Films
for Electrochemical Planarization Application**

Kambiz Dianatkah

B.E., Metallurgical Engineering University of Minnesota
Minneapolis, Minnesota

A dissertation presented to the faculty of the
Oregon Graduate Institute of Science and Technology
in partial fulfillment of the
requirements for the degree
Master
in
Materials Science and Engineering

November 1999

This thesis titled "Passivation Behavior of Copper Thin Films for Electrochemical Planarization Application" by Kam Dianatkah has been examined and approved by the following Examination Committee:

Dr. Margaret Ziomek-Moroz, Thesis Advisor
Associate Professor
Department of Materials Science and Engineering

Dr. Robert Contolini
Novellus Systems, Inc.

Dr. Milton Scholl, Associate Professor
Department of Electrical and Computer Engineering
Oregon Graduate Institute of Science and Technology

Acknowledgments

I would like to express my appreciation to my thesis advisor, Dr. Margaret Ziomek-Moroz, for her guidance, support, and patience thorough the course of this research work. I also wish to thank the other members of my dissertation committee, Dr. Robert Contolini, Dr. Milton Scholl, for their time and effort as committee members in examining my dissertation and sharing their professional opinions.

I am grateful to Dr. Rob Contolini and Dr. Steve Mayer of Novellus Systems, Inc., for their support in sponsoring this project. I would also like to thank fellow students, Hamid Faridi, David Turcio-Ortega, and Rob Davis, as well as, MSE staff member Roxanne Workman, for their help.

Finally, I would like to thank my mother, M. Nouri; my daughters, Alana and Lisa, and M. B. Taylor for their support and encouragement throughout this project.

Abstract

Passivation Behavior of Copper Thin Films for Electrochemical Planarization Application Kambiz Dianatkah, B.E

M.S., Oregon Graduate Institute of Science and Technology
November 1999

Thesis Advisor: Dr. Margaret Ziomek-Moroz

Three basic elements of electronics are 1) the device, particularly the IC, 2) the wiring structure, the interconnects in the chip and that in the printed circuit board; and 3) the joining material. Every electronic device consists of individual chips and discrete components. The ability to effectively package these components plays an important role in the overall performance of a device.

New technological innovations in electronic devices are progressing by reducing critical Dimensions and tighter photolithography. As device sizes get smaller, the electrical properties of aluminum for interconnects will not meet the new requirements for lower resistivity and greater resistance to electromigration. Copper has been considered as a replacement material for aluminum. With the increased number of layers within the chip, the importance of planarization between layers has grown greatly. In this research passivation behavior of copper thin films has been studied for electrochemical planarization (ECP) applications, versus the current mechanical planarization techniques (CMP).

The passivation behavior of copper thin films was studied in electrolytes containing a mixture of phosphoric acid (H_3PO_4) and copper ions (Cu^{2+}) using electrochemical methods and surface analysis. Physical properties of electrolytes used in this study such as electrical conductivity, viscosity, pH, and density at different temperatures were also determined. The experiments were performed on bulk copper and silicon wafers coated with copper. The hydrodynamic conditions, conductivity and viscosity of the electrolytes were found to affect copper passivation behavior of copper.

Table of Contents

Acknowledgments	iii
Abstract	iv
Table of Contents	v
List of Figures	vii
List of Tables	ix
CHAPTER 1 INTRODUCTION	1
WHY COPPER	2
PROPERTIES OF COPPER	3
CHEMICAL PROPERTIES OF COPPER	4
Acidic Solutions	4
Neutral and Alkaline Solutions	5
Corrosion Properties of Copper	6
Pourbaix Diagram	6
PASSIVATION BEHAVIOR OF COPPER	7
COPPER OXIDE PROPERTIES	9
THIN FILMS	9
METHODS OF COPPER DEPOSITION	10
Sputtering	10
Electroless and Electrolytic Deposition	11
Physical Vapor Deposition (PVD)	11
Chemical Vapor Deposition (CVD)	12
OVERVIEW OF WAFER PROCESSING	12
Damascene Processing	12
Dual Damascene	13
CHAPTER 2 RESEARCH OBJECTIVES	14
PLANARIZATION	14
Chemical Mechanical Polishing of Copper	14
HISTORY OF CMP	16
Mechanics of CMP	17
Disadvantages of CMP	17
ELECTROPOLISHING OF COPPER	17
Selection of Electrolyte	18
Kinetics of Electropolishing	19
ELECTROPOLISHING OF COPPER IN PHOSPHORIC ACID	20

ELECTROPOLISHING EFFECT ON PLANARIZATION	21
DEFECTS IN ELECTROPOLISHING	22
ROTATING DISK ELECTRODE	22
PROPERTIES OF ELECTROPOLISHED SURFACES	24
EFFECT OF ELECTROPOLISHING ON PROPERTIES OF METALS	25
CHAPTER 3 EXPERIMENTAL PROCEDURE	26
PHYSICAL MEASUREMENTS	27
Conductivity Measurement	27
Viscosity Measurements	27
pH Measurements	27
Density Measurements	27
POTENTIODYNAMIC POLARIZATION EXPERIMENTS	28
POTENTIOSTATIC EXPERIMENTS	29
OPTICAL AND SCANNING ELECTRON MICROSCOPY (SEM)	
EXAMINATION	29
SURFACE ROUGHNESS MEASUREMENTS	30
CHAPTER 4 RESULTS AND DISCUSSION	31
PHYSICAL MEASUREMENTS	31
Stability	31
Conductivity	32
Viscosity Measurement Results	35
Density Measurement Results	37
pH of the Electrolytes	38
ELECTROCHEMICAL RESULTS	49
Potentiodynamic Polarization Results	49
Effect of Phosphoric Acid Concentration	50
Effect of Dissolved Copper	51
Effect of RPM	52
Effect of Scan Rate	53
POTENTIOSTATIC POLARIZATION RESULTS	53
Surface Analysis Results and Discussion	55
CHAPTER 5 CONCLUSIONS	62
Future Work	63
REFERENCES	64

List of Figures

Figure 1.	Illustration of a typical silicon chip	1
Figure 2.	Potential-pH Diagram of Copper in Water System, Modified Diagram ⁸	7
Figure 3.	Idealized current density versus applied voltage for many common electrolytes ¹³	8
Figure 4.	Degree of planarity	15
Figure 5.	Schematic diagrams of processes involved in electrochemical planarization, a) before planarization, b) after planarization	15
Figure 6.	Schematic of a polarization cell ³	28
Figure 7.	Conductivity measurements vs temperature in 45% H ₃ PO ₄	32
Figure 8.	Conductivity measurements vs temperature in 60% H ₃ PO ₄	33
Figure 9.	Conductivity measurements vs temperature in 65% H ₃ PO ₄	33
Figure 10.	Conductivity measurements vs temperature in 75% H ₃ PO ₄	34
Figure 11.	Conductivity measurements vs temperature in 85% H ₃ PO ₄	34
Figure 12.	Viscosity measurements vs temperature in 65% H ₃ PO ₄	35
Figure 13.	Viscosity measurements vs temperature in 75% H ₃ PO ₄	36
Figure 14.	Viscosity measurements vs temperature in 85% H ₃ PO ₄	36
Figure 15.	Anodic polarization of copper disk electrode rotated at 9 rpm in 60%, 65%, 75% H ₃ PO ₄ at a copper concentration of 1.2 M Cu ²⁺	50
Figure 16.	Anodic polarization of wafer coated with thin copper film in 65% H ₃ PO ₄ , rotated at 9 RPM with 0.8 M and 1.2 M Cu ²⁺	51
Figure 17.	Anodic polarizarion of copper disk electrode rotated at 100, 200, and 300 rpm in 75% H ₃ PO ₄ and 1.2M Cu ²⁺	52
Figure 18.	Anodic polarization curves of copper in 65% H ₃ PO ₄ and with 1.2M Cu ⁺⁺ , 10 mv/s and 20 mv/s	53
Figure 19.	Potentiostatic polarizarion of wafer in 65% H ₃ PO ₄ with 1.2M Cu ⁺⁺ , E _{app}	54
Figure 20.	Potentiostatic polarizarion of copper in 65% H ₃ PO ₄ and 1.2M Cu ⁺⁺ E _{app}	54
Figure 21.	EDX results of the base wafer coated with copper	57
Figure 22.	EDX results of the wafer following the potentiostat test at 2.2V	57
Figure 23.	Optical micrograph of base wafer 200x	58
Figure 24.	SEM micrograph of a wafer 1000x (a) base, (b) following potentiodynamic test	58
Figure 25.	SEM micrograph of a wafer 1500 following potentiostatic test (a) 2.2V, (b) 2.4V	59
Figure 26.	Surface roughness data after potentiostatic tests at 2.0V	61
Figure 27.	Surface roughness data after potentiostatic tests at 2.2V	61

List of Tables

Table 1.	Comparison of some critical properties of copper versus aluminum used in the electronic industry	3
Table 2.	Density pH measurements of H_3PO_4 and Cu^{2+} , Temp = 25°C	38
Table 3.	Slope of Conductivity Plots	38
Table 4.	Slope of Viscosity Plots	39
Table 5.	Physical Measurements	39
Table 6.	Conductivity and Viscosity Measurements of Electrolytes containing 45% H_3PO_4 with 0.25 M Cu as a function of temperature	40
Table 7.	Conductivity and Viscosity Measurements of Electrolytes containing 45% H_3PO_4 with 0.5M Cu as a function of temperature	40
Table 8.	Conductivity and Viscosity Measurements of Electrolytes containing 45% H_3PO_4 with 0.76M Cu as a function of temperature	40
Table 9.	Conductivity and Viscosity Measurements of Electrolytes containing 45% H_3PO_4 with 1M Cu as a function of temperature	41
Table 10.	Conductivity and Viscosity Measurements of Electrolytes containing 50% H_3PO_4 with 0.395M Cu as a function of temperature	41
Table 11.	Conductivity and Viscosity Measurements of Electrolytes containing 50% H_3PO_4 with 0.52M Cu as a function of temperature	41
Table 12.	Conductivity Measurements of Electrolytes containing 50% H_3PO_4 with 0.65M Cu as a function of temperature	42
Table 13.	Conductivity and Viscosity Measurements of Electrolytes containing 50% H_3PO_4 with 1.05M Cu as a function of temperature	42
Table 14.	Conductivity and Viscosity Measurements of Electrolytes containing 50% H_3PO_4 with 1.57M Cu as a function of temperature	42
Table 15.	Conductivity Measurements of Electrolytes containing 50% H_3PO_4 with 2.63M Cu as a function of temperature	43
Table 16.	Conductivity and Viscosity Measurements of Electrolytes containing 60% H_3PO_4 with 0.56M Cu as a function of temperature	43
Table 17.	Conductivity and Viscosity Measurements of Electrolytes containing 60% H_3PO_4 with 0.7M Cu as a function of temperature	43
Table 18.	Conductivity and Viscosity Measurements of Electrolytes containing 60% H_3PO_4 with 0.7M Cu as a function of temperature	44
Table 19.	Conductivity and Viscosity Measurements of Electrolytes containing 60% H_3PO_4 with 0.84M Cu as a function of temperature	44
Table 20.	Conductivity and Viscosity Measurements of Electrolytes containing 60% H_3PO_4 with 1.686M Cu as a function of temperature	44
Table 21.	Conductivity and Viscosity Measurements of Electrolytes containing 60% H_3PO_4 with 0.84M Cu as a function of temperature	45
Table 22.	Conductivity and Viscosity Measurements of Electrolytes containing 65% H_3PO_4 with 0.29M Cu as a function of temperature	45

Table 23.	Conductivity and Viscosity Measurements of Electrolytes containing 65% H ₃ PO ₄ with 0.73M Cu as a function of temperature	45
Table 24.	Conductivity and Viscosity Measurements of Electrolytes containing 65% H ₃ PO ₄ with 1.74M Cu as a function of temperature	46
Table 25.	Conductivity and Viscosity Measurements of Electrolytes containing 70% H ₃ PO ₄ with 1.5M Cu as a function of temperature	46
Table 26.	Conductivity and Viscosity Measurements of Electrolytes containing 75% H ₃ PO ₄ with 0.15M Cu as a function of temperature	46
Table 27.	Conductivity and Viscosity Measurements of Electrolytes containing 75% H ₃ PO ₄ with 0.62M Cu as a function of temperature	47
Table 28.	Conductivity and Viscosity Measurements of Electrolytes containing 75% H ₃ PO ₄ with 0.78M Cu as a function of temperature	47
Table 29.	Conductivity and Viscosity Measurements of Electrolytes containing 75% H ₃ PO ₄ with 0.94M Cu as a function of temperature	47
Table 30.	Conductivity and Viscosity Measurements of Electrolytes containing 75% H ₃ PO ₄ with 1.25M Cu as a function of temperature	48
Table 31.	Conductivity and Viscosity Measurements of Electrolytes containing 75% H ₃ PO ₄ with 1.87M Cu as a function of temperature	48
Table 32.	Conductivity and Viscosity Measurements of Electrolytes containing 85% H ₃ PO ₄ with 0.2M Cu as a function of temperature	48
Table 33.	Conductivity and Viscosity Measurements of Electrolytes containing 85% H ₃ PO ₄ with 0.6M Cu as a function of temperature	49
Table 34.	Potentiodynamic Summary	55
Table 35.	Potentiostatic Summary	55

CHAPTER 1

INTRODUCTION

Aluminum and its alloys have been predominantly used for interconnects in very large scale integrated (VLSI) and ultra large scale integrated (ULSI) circuits¹. However, for the sub-micron features of devices, problems such as high resistance, poor electromigration reliability and adaptability to damascene processes have been encountered. For better electrical and corrosion properties, alternative materials such as copper and silver have been considered to replace aluminum.

Aluminum is sometimes alloyed with silicon to reduce interdiffusion with a substrate or with copper to strengthen the metal and to reduce electromigration. Patterning interconnect materials are achieved by wet etching or reactive ion etching. Metallization is performed to obtain unique properties for each layer in a wafer.

In practice, electronic devices are becoming smaller and denser as more elements are placed on a chip (also called a die). Figure 1 shows a scheme of a typical silicon chip.

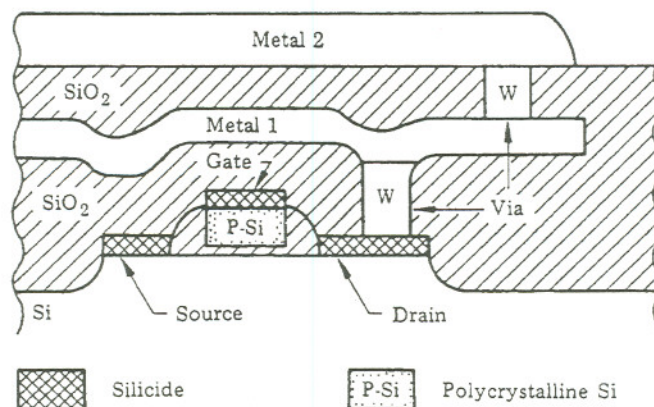


Figure 1. Illustration of a typical silicon chip¹

The substitution of Al-based metallization (Metal 2 in Figure 1) by copper requires a new approach in material selection and manufacturing technology. One of the major concerns for using copper is copper-silicon interdiffusion. This is controlled by deposition of a thin layer of silicon nitride or other diffusion barrier materials such as tantalum, tantalum-based alloys, and tantalum nitride. A thin film of copper is then deposited by physical vapor deposition (PVD) on the diffusion barrier layer². Tantalum is an attractive alternative as a diffusion barrier since it has a high melting point and is immiscible with copper. Tantalum also reacts with other metals to form a strong metal-metal bond. Tantalum is beneficial to copper metallization since it forms high temperature stable ohmic contacts². In addition, it provides an amorphous ultra thin barrier free from extended defects² for protection against general, localized and environmental induced corrosion.

Processing of copper-based metallization is generally contingent upon the use of damascene structures, which are generally planarized by chemical mechanical polishing (CMP). In this thesis, applications of basic corrosion studies for developing a complementary method to CMP, i.e, electrochemical planarization is being studied.

WHY COPPER

The transition from aluminum to copper interconnects in the semiconductor industry has rapidly accelerated during 1999. The use of copper as a material for a chip interconnect offers several advantages over aluminum-based alloys mainly due to two major factors, lower resistivity and superior electromigration resistance³. The resistivity that copper offers relative to aluminum is a critical issue, which may result up to a 40% increase in speed of microprocessors. Most current integrated circuit metallization designs use aluminum alloys in part or entirely. For example, aluminum has a resistivity of 2.66 $\mu\Omega$ -cm. Other metals that have lower resistivity than aluminum are copper, gold and silver^{3,4,5}. Table 1 compares some critical properties of copper versus aluminum used in the electronic industry³.

Table 1. Comparison of some critical properties of copper versus aluminum used in the electronic industry

	Aluminum (Al)	Copper (Cu)
Resistivity ($\mu\Omega\text{-cm}$)	2.66	1.67
Electromigration	Poor	Good
CVD Processing	?	Available

In order to use copper as an interconnect, susceptibility of copper to corrosion and electromigration must be determined as well. Silver and gold are potential replacement candidates for aluminum; however, electromigration issues must be examined first¹². Based on evaluation of all pertinent properties and economic analysis³, copper and aluminum are the preferred choices. Copper has higher melting point 1356 K compare to 933 K for aluminum which may result in better resistance to electromigration^{2,3,4} and can handle higher current densities, e.g. 5×10^6 A/cm².

PROPERTIES OF COPPER

Copper has been one of the most important metals used in advancement of technology. Copper usage is second only to iron^{4,5}. The discovery of copper dates back to prehistoric times, with use covering 7000 years. Copper is the only metal found in its metallic state ready to produce tools. Part of the reason it was used so early historically is that it is relatively easy to shape. Copper softness is due to its face centered cubic atomic structure. After it is refined, copper is alloyed with other metals to make it harder than pure copper. For example, brass is an alloy of copper and zinc and bronze is an alloy of copper and tin.

Copper is the first element of group IB of the periodic table, has atomic number 29 and occurs in two isotopes, ⁶³Cu and ⁶⁵Cu³. It is reddish with a bright metallic luster, malleable and ductile. Copper is a good conductor of heat and electricity (second only to silver in electrical conductivity). Its high electrical and heat conductivity is due to unique electronic configuration of 2-8-18-1. This electronic configuration suggests a closed stable of 18 electrons but the

d orbitals participate in metallic bonding by promoting a *d* electron into the higher energy orbital outermost quantum level⁵. The *d* electron often participate in thermal and electrical conduction for copper.

The presence of any impurities lowers copper's conductivity. The presence of 100-500 parts per million (ppm) oxygen does lower copper's conductivity somewhat, but prevents most other impurities entering its solid solution during processing³. Copper oxides are unstable relative to other metals since low free energy of formation reduces very easily and they are less polar. Copper has higher ionization energy and smaller ionic radius³.

Copper has great commercial importance since over seven million tons are used annually. For example copper is used as wire, coinage metal, tools, electrical conductor testing and casting alloys. A principle use is in the electrical and electronic industries for interconnect applications⁴.

CHEMICAL PROPERTIES OF COPPER

Acidic Solutions

Copper does not generally displace hydrogen in acid solutions and therefore, it is virtually unattacked in non-oxidizing conditions. Copper dissolves in acid solution that contain dissolved oxygen but can be used in most mild acids (non-oxygenated)^{5,6}.

Oxidizing acids, such sulfuric and nitric acids attack copper according to the reactions listed below:



The reaction of Copper with H_2SO_4 proceeds as follows:



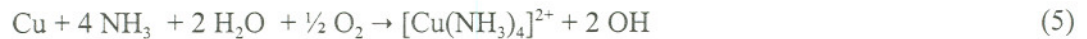
Neutral and Alkaline Solutions

Copper and copper alloys are resistant to alkaline solutions^{6,7} over a wide range of conditions, but are attacked in concentrated bases, especially at high temperatures. For example, ammonia forms complexes with copper increasing its susceptibility to general corrosion and stress corrosion cracking.

Dissolution of copper in low concentration NH_4OH proceeds as follows:



Dissolution of copper and formation of the $[\text{Cu}(\text{NH}_3)_4]^{2+}$ complex ion occurs in high concentrations of NH_3 and water. This reaction requires the presence of oxygen⁶ and goes on as follows:



The type II copper complexes are formed by reaction with metallic copper as follows:



When oxygen is still present in the system, complex $[\text{Cu}(\text{NH}_3)_2]^{2+}$ further reacts forming $[\text{Cu}(\text{NH}_3)_4]^{2+}$:



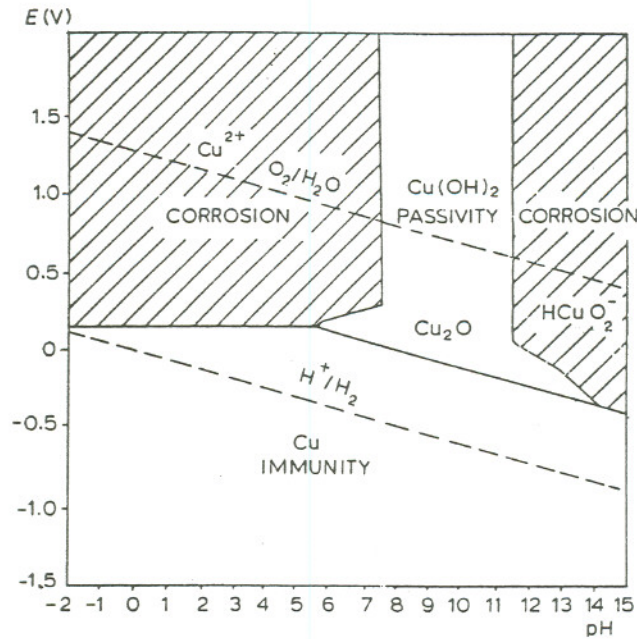
The reaction represented by Equation 5 is faster than the reaction represented by Equation 6. The dissolution of copper occurs according to Equation 5; however, reaction represented by Equation 6 also occurs, but in the diffusion layer.

Corrosion Properties of Copper

Copper naturally occurs in the environment and it is naturally obtained by reduction of its compounds. Based on the electrochemical series⁸, it is not chemically very reactive and oxidizes slowly in atmosphere at room temperature. It has a relatively noble potential based on the EMF series and galvanic series^[5]. Copper compounds are highly colored. Very small amounts of copper added to a solution may cause considerable corrosion of more anodic metals elsewhere in a system⁸. Copper and copper alloys are more corrosion resistant than copper itself due to more protective and stable film formation. Copper only tarnishes in the presence of hydrogen sulfide. Corrosion resistance of copper is not affected by humidity significantly. Localized corrosion such as pitting has been observed in copper and copper alloys^{8,9} in cold water and to much lesser extent in hot water. The major contributing factors for the formation of pits are contributed by annealing processes and impurities within the microstructure.

Pourbaix Diagram

The potential-pH diagram is basically designed for a metal/water system which shows the condition of oxidizing power versus the acidity or alkalinity (pH)^{8,9,10}. A traditional Pourbaix diagram describes the reaction of a typical metal in a water system to indicate regions of immunity, corrosion, and passivation. The diagram is constructed based on the Nernst equation where the component of concentration (activity) is drawn as contours to divide each region in more detail. The Pourbaix diagram is based on potential of a metal vs hydrogen electrode and is plotted against pH of an electrolyte. pH measurements are basically obtained using a high impedance pH meter. All possible reactions are shown in the diagram to indicate where each phase of a metal is present. Figure 2 shows a typical diagram for the copper and water system. There are three main regions within the Pourbaix diagram: corrosion, where metal in the form of cations and anions is present, passivity or passivation region where a stable metal oxide generally forms on the metal and finally, a region in which metal itself is present and no reaction occurs.



Within the Pourbaix diagram, two lines are also drawn where stability of hydrogen and oxygen gases and water is indicated to assist in potential reactions that may be expected. The regions that allow for thermodynamically stable compound are referred to as the passive region.

Figure 2. Potential-pH Diagram of Copper in Water System, Modified Diagram⁸

PASSIVATION BEHAVIOR OF COPPER

Passivation or oxidation occurs due to impurities present in thin films. The grain boundaries which separate grains must accommodate the discontinuities between misdirected lattices. This resulting disorder region serves as a sink for impurities and an area ready for fast oxidation. Water is considered a major impurity which affects the rate of oxidation at low temperature^{8, 11, 12}. Measurement of thin film growth is critical to determine the role of passivation. By measuring thin film growth, the effect of temperature, oxygen, metal structure, time and impurities could be determined.

Figure 3 shows an idealized polarization curve of a typical passivating metal in an electrolyte, where current density is plotted versus applied potential relative to a reference electrode. This figure is critical in understanding the passivation of metal and is similar to the electrochemical passivation behavior of copper in phosphoric acid.

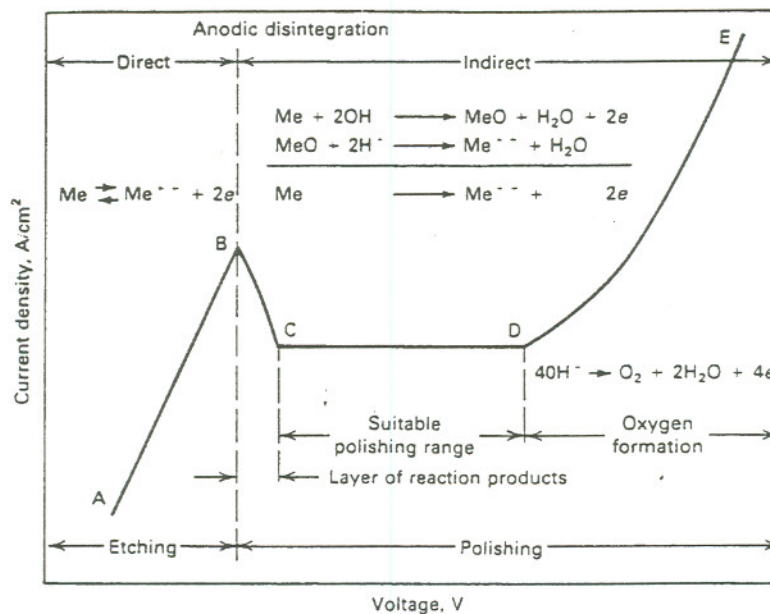


Figure 3. Idealized current density versus applied voltage for many common electrolytes¹³

Figure 3 is basically divided into 4 regions of interest: Region 1 is defined by line AB, where only metal dissolution occurs and most of metal surface remains fairly unchanged. Region 2 is shown by line BC where active-passive behavior occurs. The next significant area, pertinent to this thesis, is shown as region CD where it represents the polishing zone. The best polishing occurs near or just beyond point D. Theoretically, better polishing results should be obtained past point D, where oxygen may not get trapped on the surface to form pits^{8,11,13}. Between point C and D, the current remains fairly constant while potential increases. The length of this line is dependent on the passivating metal behavior and the electrolyte. The final region is referred to as a transpassive zone, where the passive film begins to breakdown and metal dissolution occurs

followed by oxygen evolution. Pitting is associated with this region since localized corrosion increases by formation of many gas bubbles and high acidity. A review of possible reactions of copper in phosphoric acid is shown in Chapter 2 under the electropolishing section. As it can be observed, the limiting current density, I_L (line CD) depends on concentration of an electrolyte, viscosity and density of solution and diffusivity of species present. Also, at I_L , flat region cautioned by concentration polarization where electropolishing occurs, an increase in current density with increasing RPM is characteristic of such electrochemical processes.

COPPER OXIDE PROPERTIES

Copper oxides are unique in that they can be reduced above the hydrogen evolution potential⁹. Generally, a constant current is applied according to $i \times t = \text{number of coulombs}$ in order to reduce copper oxide. In this method, CuO can be reduced to Cu₂O above the hydrogen evolution potential. There are two requirements for this cathodic reaction, exclusion of oxygen, and use of an electrolyte that does not dissolve the oxide film^{11,12}.

THIN FILMS

Thin films function as insulators and passivation coatings or electrical conductors used in interconnect devices or passive components such as resistors, capacitors and inductors. Thin films will continue to be an area of major focus for development in fine-line patterning and multilayers for the electronic industry. Thin films are expressed in terms of their thickness¹⁰ and range in thickness from a few angstroms to several micrometers. Thin films are referred to as the metallization layer, as in the case of copper or aluminum metallization layer following sputtering, PVD or CVD operations. Thin films of organic polymer, such as polyimides are used as interlayer dielectrics or in multichip modules.

Substrates for thin films include of metals, ceramics, metal-ceramic composites and plastics. The substrates serve the following functions:

1. Provide mechanical support for interconnecting and assembly devices.

2. Provide means for electrical insulation on which passive devices and conductor traces are deposited and patterned.
3. Provide a thermal medium for conducting and transferring heat from the devices.
4. Provide dielectric layer to control impedance, crosstalk and signal propagation for high speed circuits¹⁰.

Currently, thermal conduction for heat dissipation is one of the major focus. Substrates are selected based on the following major properties: electrical, chemical, physical and thermal. Performance and reliability are the major keys when considering a substrate.

In addition to metallic thin films, non-metallic thin films of different types are now being used in advanced commercial products^[4]. For example, polycrystalline silicon (polysilicon) is a common structural material in micro-electro-mechanical systems (MEMS) such as pressure sensors and accelerometers.

METHODS OF COPPER DEPOSITION

There are four main common methods used in the industry for the deposition of copper on various substrates^{2,14,15}: Sputtering, Electroless and Electrolytic Deposition, Physical Vapor Deposition, and Chemical Vapor Deposition.

Sputtering

A blanket of copper is deposited by sputtering for features with less than 25 μm line width and 50 μm spacing between lines. The copper film is then photo-patterned with resist, followed by a wet etch to remove the unwanted copper. This technique does not define more aggressive features due to inherent undercutting associated with wet etching. In the sputtering technique, the surface of a solid target is vaporized by bombarding it with inert gas ions, sometime accelerated by a potential of 500 to 5000 volts.

Electroless and Electrolytic Deposition

Wet plating of metallic layers encompasses processes where coatings are deposited on a substrate in a liquid, usually aqueous, containing the appropriate metallic ions, oxidizers, and reducers. The deposition often functions by ionic discharge consisting of the electrochemical processes of cathodic and anodic reactions. The plating process can introduce organic compounds into the metal coating; although, this can be minimized by controlling bath composition¹³.

Thin film copper coatings can be grown autocatalytically without an applied electric field, through a reduction of a metal ions in the plating bath by the immersed substrate. This method is known as a chemical displacement. Another known autocatalytic process occurs in an electroless plating bath which involves the deposition of metal from a plating bath containing metal ions with a reducing agent. This process differs from the chemical displacement method in that no significant reaction occurs within the volume of the liquid and the depositing metal catalyzes further deposition, so that a thicker film can be grown. In most cases, it is usually necessary to activate non-metallic substrates by chemical treatment in order for them to generate a catalytic reaction.

Physical Vapor Deposition (PVD)

In PVD process, the coating material is physically converted into a vapor and then made to condense on the surface of the substrate without going into any fundamental chemical change in the process. Vacuum evaporation covers the methods where a coating is thermally vaporized by heating or by electron beam bombardment.

In the PVD process, the deposition process takes advantage of an ionized fraction of the condensing vapor, the process is described as "ion-aided." Ion plating and ionized cluster beam deposition are the two techniques based on this principle. Physical vapor deposition reflow offers lower cost with less impurities and better electromigration properties compared to chemical vapor deposition (CVD).

Chemical Vapor Deposition (CVD)

Chemical vapor deposition is a coating method by means of chemical reaction and is classified according to the type of chemical reactions involved. In a decomposition reaction, a gaseous compound such as XY may be decomposed into solid condensate X and a gaseous Y when placed in contact with a cold surface². For small features in the sub-micron level, chemical vapor deposition and sputtering techniques used in the electronic industry may create difficulties such as incomplete filling of sub-micron holes. Ideally the coating is preferred to be covalently bonded to the substrate, giving very good adhesion.

OVERVIEW OF WAFER PROCESSING

Damascene Processing

Fabrication of copper interconnects has generally been established today. Damascene and dual damascene process are primary methods. The traditional damascene processes is the application of interlacing copper or gold on another metal to produce beautiful decorative. The art of damascene was practiced for centuries by Egyptians, Greeks, and Romans. Around the XV century the art work became popular worldwide.

When aluminum is used in fabrication of interconnects, one could put down a photoresist mask on top of the deposited aluminum and plasma etch away from the unprotected aluminum. Since copper cannot be etched, one could use a process called 'damascene' by making a trench and deposit the copper into it².

Dual Damascene

The dual damascene structure is constructed by forming vias and trenches in the dielectric layer. A layer of photoresist is coated on the wafer and the via patterns are formed in the photoresist with lithography^{14,15}. The processing step consists of etching the vias followed by another lithography process. The "Dual-Damascene" method is used to etch the trenches, fill them electrolytically with copper, then mechanically polish away the excess metal using a chemically active slurry. In the Dual-Damascene process, vias and metal interconnects are formed concurrently. The major difference with single layer damascene is the lower cost since fewer steps are required.

CHAPTER 2

RESEARCH OBJECTIVES

In this thesis, applications of basic corrosion studies are applied for developing electrochemical planarization technique. The passivation behavior of copper thin films in a mixture of phosphoric acid (H_3PO_4) and copper ions for planarization applications is Investigated.

PLANARIZATION

Smoothing or milling the surface of a metal is referred to as planarization in the electronic industry^{3,16}. Conventional methods used to achieve planarization are Spin-on-glass (SOG) and chemical mechanical polishing (CMP). The reason for performing planarization is to reduce the step heights that metal lines have to traverse. Enhanced chip productivity and yield due to improved planarization are the goals in this segment of the semiconductor capital equipment market. Figure 5 shows an example of the typical wafer surface before and after planarization.

Chemical Mechanical Polishing of Copper

CMP is an abrasive process used for polishing the surface of the wafer flat. It can be performed on both oxides and metals³. It involves the use of chemical slurries and an abrasive action to polish the surface of the wafer smooth. The smooth surface is required for photolithographic depth of focus, and also to ensure that interconnects are not deformed over contour steps.

Chemical Mechanical Polishing (CMP) of Copper is a method of achieving global film planarization, using technology adopted from the precision grinding and lapping industry. Metal CMP is capable of producing extremely flat surfaces on materials such as tungsten, aluminum or silicon using aluminum oxide, silica, or cerium oxide abrasives in a pH controlled solution.

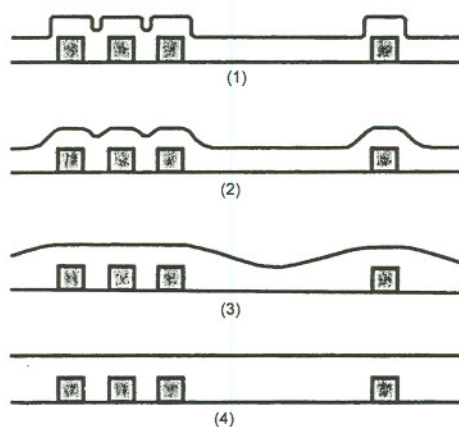


Figure 4. Degree of planarity³

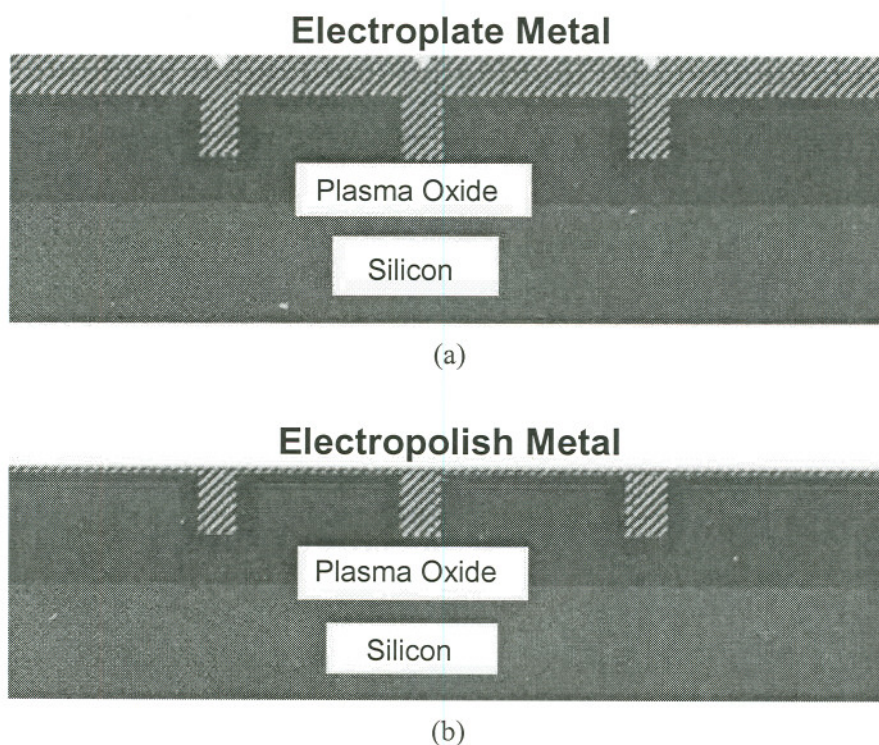


Figure 5. Schematic diagrams of processes involved in electrochemical planarization, a) before planarization, b) after planarization¹⁷

HISTORY OF CMP

Although polishing and planarization methods have been used for centuries, it was not until the mid-1980s that chemical-mechanical polishing (CMP) was first integrated into semiconductor technology. Integration of CMP technology into chip production has enabled higher yield processes and more reliable products with more than two layers of metal interconnect wiring in the production of higher density VLSI and ULSI chips^{3,16}.

Thus far CMP has been one of the only commercial technique to produce globally planar oxide surfaces. The ability to planarize both metal and oxide layers quickly led to the conclusion that one might obtain layer after layer of interconnects by replicating the identical process sequence without increasing the amount of topography and suffering compounded yield degradation. Furthermore, by reducing step heights, narrower and narrower minimum line widths have been possible. The benefits of CMP to lithography process yields have been significant.

The first generation of CMP tools used by the semiconductor industry were modified silicon wafer polishing machines. These polishing tools consist of a polishing arm with a wafer carrier and a rigid polish platen. The wafer is held device side down, and pressed into a polish pad that is affixed to the platen with adhesive. The carrier presses the wafer into the pad mid-way between the center of the platen and the edge of the platen. Both the platen and the carrier rotate, typically in the same direction. Slurry is dispensed on the pad near the center of the pad, and centripetal force and carrier motion distribute the slurry around the upstream periphery of the carrier. The surface roughness and pad porosity transport the slurry underneath the wafer.

Due to the initial high cost of ownership (CoO) for wafer CMP in semiconductor manufacturing, continuous improvements were made to the first-generation CMP tools. Specific areas of improvement were reliability and throughput. Further improvement of this first generation CMP led to the development of higher raw throughput second generation tools with multiple wafers being polished simultaneously on a single polish platen. However, multiple wafers being simultaneously polished on a single pad and platen increased the risk to wafer yield, leading to the development of multi-headed single-wafer-per-platen polish tools.

Mechanics of CMP

Chemical/mechanical polishing utilizes a chemically active liquid slurry containing very fine particles to planarize the surface of a wafer³. The slurry coats the top of the wafer and is pressed between the wafer and a compliant circular rotating pad. The surface of the pad in contact with the slurry is not smooth, and contains grooves. The liquid in the slurry is formulated to have a slight etching effect. As the slurry flows over the wafer surface, the suspended particles abrade the surface and the liquid in the slurry etches the abraded area. The process is somewhat like using a rotary buffer to polish the finish on a car. The overall objective is to understand how the achievable flatness is related to the many variables that might be controlled in the process, for example the pressure on the pad, the rotation speed, the sizes of the particles in the slurry, the pad conditioning, the chemistry of the liquid used in the slurry, etc.

Disadvantages of CMP

The problems associated with CMP process are wafer dishing and feature recess. Dishing is excessive removal of material in large surface area pad features relative to smaller surface-area lines (Figure 5). Another associated problem with CMP is sometimes excessive removal of metal that may involve removal of other materials depending on the effectiveness of the pad/slurry combination³. Another drawback of CMP operation is that the surface of wafer can not be observed during the processing².

ELECTROPOLISHING OF COPPER

Electropolishing processes has the potential to replace a number of operations such as mechanical polishing and etching processes. It is widely used in many branches of science and technology and is essentially the reverse of electroplating. Electropolishing of metals is achieved by operating at the mass-transfer limited rate of dissolution. The mass transfer depends on the metal and the electrolyte.

Electropolishing is accomplished by connecting a copper or metal electrode to the anode of a DC power supply or a potentiostat and by placing the sample that needs to be polished to the negative terminal (cathode). In the case of potentiostatic connection, a three electrode system is used and a working electrode is connected to the metal which is going to be polished (anode), a counter electrode such as platinum or graphite completes the circuit, and finally a reference electrode to measure the potential of working electrode. The electrical reaction causes ionic conduction resulting in the removal of particles of metal from the anode. During the electrolytic process, the products of the anodic metal dissolution react with the electrolyte to form a film at the surface of the metal.

Selection of Electrolyte

Anodic dissolution of a metal depends on its properties, surface state, the composition of electrolyte, and the process conditions (temperature, current density, stirring)¹³. The ideal electrolyte is required to achieve optimum polishing conditions is usually associated with strong anodic polarization in order to form passivating films of low conductivity. The films must also dissolve in the electrolyte in order not to inhibit the anodic process. Electrolytic polishing processes occupy an area between anodic etching (dissolution) and anodic oxidation region. During etching, metal dissolves in the electrolyte while in the anodic oxidation, the oxide film is not dissolved. The thickness of anodic film or passivating layer may change pending on current and electrolyte composition. An idealized electrolyte must satisfy the following requirements^[13]:

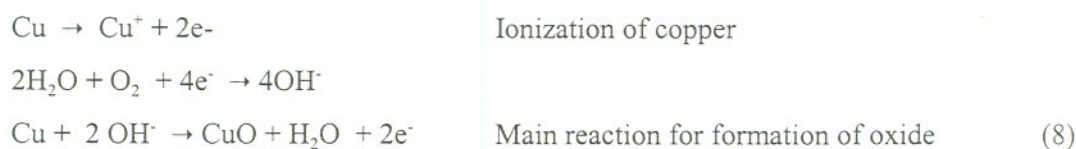
1. High quality polishing at low voltages and current densities.
2. Large range of current densities and temperatures.
3. Stability and long service life.
4. Does not to dissolve the metal while no current is flowing.
5. Inexpensive and readily available and must meet safety requirements.
6. After use be recoverable by addition of necessary components.
7. Ohmic resistance or IR drop should be low to obtain the required current density at low voltage.
8. Must possess good throwing power, i.e, a sample with complex geometry should dissolve uniformly on the entire surface.

Kinetics of Electropolishing

The electropolishing kinetics is influenced by polishing current, temperature of electrolyte, polishing time, surface preparation, agitation or stirring of electrolyte (to remove products from the anode layer and remove bubbles), as area of cathode (must be larger to obtain optimum polishing rate). Since the electropolishing process is referred to as a diffusion controlled process, the effect of stirring or rotating specimen significantly increases the rate of reaction. Under steady state conditions, anodic reaction products build up on the surface and may interfere with the polishing process¹⁸. Stirring or use of rotating disk electrode maintains a stable temperature, homogeneous electrolyte and prevents build up of corrosion products on the surface unless the specimen is polarized in a passivating area.

Oxide film can form during electropolishing of copper¹⁹. The thickness of oxide film is dependent on the nature of metal, electrolyte composition, rate of electropolishing and conditions that exist during electropolishing. In electropolishing, due to the concentration gradient from diffusion of anodic dissolution product from the anode to the bulk, with irregular samples it is possible to surface etch without polishing. In the case where there is no surface film present¹², a non-uniform current distribution would be observed.

If the oxide film formed during electropolishing shows ionic conductance, the electrochemical oxidation (anodic/active passive behavior) is followed by metal dissolution and oxygen evolution. During electropolishing of copper in phosphoric acid ($\text{pH} < 2$)^{19,20}, when the final polarization area after polishing is reached, a reaction occurs which results in discharge of hydroxyl ions with evolution of oxygen²¹:



Generally, the potential during this reaction does not change a great deal with increasing current density. Oxygen evolution may also take place as a result of oxygen-containing anions such as phosphate and sulfates forming higher oxygen compounds and eventually transitioning to lighter containing-oxygen compounds.

ELECTROPOLISHING OF COPPER IN PHOSPHORIC ACID

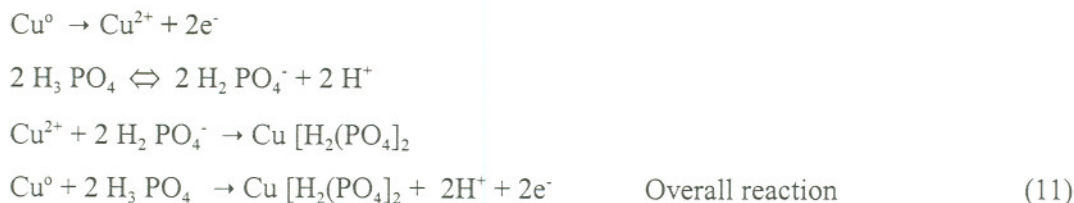
Electropolishing of metals usually takes place at a limiting current which is determined by the physical properties of the polishing solution, the initial roughness of the metal electrode, geometry, and the hydrodynamic factors. Ortho-phosphoric acid is widely used for the electropolishing of copper and its alloys^{13,20}. Electrolytic polishing is smoothing or brightening of a metal surface by anodic dissolution in an electrolytic cell. Generally, anodic dissolution roughens the surface of the metal; however, bright smooth surfaces can be obtained with the right electrolyte and current range and temperature. The following two general anodic reactions are proposed for the electrochemical polishing of copper in phosphoric acid^[18]:

Reaction type 1^{20,21} :



Reaction type 2 is similar to type 1 reaction for electropolishing of copper in phosphoric acid, however, the type 2 reaction does not include any reaction with water. The partial and overall reactions are shown below^{21,22}:

Reaction type 2



Current density is usually determined by the diffusion rate of metal ions from the surface of the electrode into the bulk solution. It will be discussed in a later section that electrochemical reaction for copper in the phosphoric acid is under diffusion control. The major factors that influence electropolishing are solution flow velocity, heat, passivity behavior of metal, viscosity and conductivity of the solution. Additional dissolved copper in the phosphoric acid will also greatly influence the physical properties of the electrolyte such as viscosity, conductivity and density.

ELECTROPOLISHING EFFECT ON PLANARIZATION

Surface roughness during passivation and electropolishing may alter significantly based on stability of film formation during the passivation stage. Since on the metal surface, there are cavities and crevices¹³. These areas require much higher current densities in order to obtain uniform polished surfaces. During the electropolishing, a liquid layer with corrosion products from anodic reactions forms on the metal and has a higher viscosity than the bulk fluid¹⁹. The thickness of this layer varies throughout the anode surface area and it is greater in the crevices. Greater thickness of this more viscous layer is a result of higher current density and the differential concentration gradient between the anode and electrolyte.

If one assumes a uniform dissolution rate of the anode, the leveling of rough surfaces in terms of peaks and crevices follows a sequence where most peaks are dissolved in all directions while crevices are dissolved preferentially in one direction. In addition, the diffusion process during electrolytic polishing is faster at the peaks than in the crevices. If uniform dissolution is to be maintained, the creation of new roughness via selective etching of the surface can be avoided by selection of a more idealized electrolyte and process optimized conditions. Surface leveling, or planarization, should occur due to preferential dissolution of peaks^{23,24}; however, in some cases surface non-uniformity may increase due to localized etching. Therefore, careful use of electropolishing is required since under optimum polishing conditions, the surface layer of material must be dissolved uniformly, regardless of heterogeneities on the surface.

DEFECTS IN ELECTROPOLISHING

Pitting as a result of incorrect electrolyte or oxygen bubbles trapped on the surface could occur and blemishes due to intermetallic compounds or inherent defect on the metal surface may occur. Finally scratches after inadequate surface preparation may be found following polishing^{13,20}.

ROTATING DISK ELECTRODE

In the study of corrosion of copper, the hydrodynamic effects of the electrolyte plays a critical role in a diffusion control process where transfer of reactants is the rate determining step in the metal corrosion process¹⁸. In this investigation, corrosion behavior and passivation of copper is used to select an ideal electrolyte and to determine the ideal potential range for copper removal for planarization. Since the electrochemical process is under diffusion control, the flow regime or hydrodynamic effects, kinematic viscosity, and concentration of electrolyte are the main variables that affect the removal rate of copper during planarization. The rotating disk electrode was selected to study the hydrodynamic effect of copper electrode since the flow regime assumed to be laminar flow. Generally, the rotating disk electrode is superior to static systems in order to study the kinetics of heterogeneous reactions. This is due to the fact that the diffusion layer is independent of the disk radius so that the change in the type of the control of a reaction is well defined and it appears over the entire disk area.

For electrolytes in a diffusion control led process where a stationary condition exists and the process is dependent on mass transfer of solute in a liquid, the following equation governs the process:

$$V \text{grad } C = D \Delta C \quad (11)$$

Where D = diffusivity, ΔC = concentration gradient and V = Liquid velocity vector.

The diffusion layer is also controlled by removal of solute due to the electrochemical reaction and the boundary layer due to changing velocity of the electrolyte.

The following equations proposed by Levich describe the system in a flow pattern (laminar flow) using the rotating disk electrode¹⁸:

$$j = D \left(\frac{dc}{dt} \right)_{x=0} = \frac{D(C_0 - C_1)}{\delta} \quad (12)$$

$$\delta = 1.61D^{1/3} \nu^{1/6} \omega^{-1/2} \quad (13)$$

where

δ = diffusion layer thickness

j = diffusion flux

D = diffusion coefficient of a reactant C_0

C_0 = Concentration at the disk surface

C_1 = Concentration in bulk

ν = Kinematics viscosity

ω = Angular velocity of disk.

Equation 12 is also identical to the well known Nearst equation; however, the diffusion layer thickness, δ is a constant.

If the rate of reactant transport is slower than the rate of the chemical reaction, then $C_1 = 0$ and reaction occurs under diffusion control conditions. In the case where reaction rate is slower than the rate of transport, $C_1 = C_0$ and the process is under activation control where corrosion film is not present and the metal continuously corrodes.

For a smooth disk in a laminar flow regime, the rotating disk electrode's Reynolds numbers may be calculated by^{18,22}:

$$Re = r^2 \omega / \nu; \text{ where } r = \text{disk radius}$$

This equation assumes that the surface area of the disk is infinitely large.

In a diffusion process, where $C_1 = 0$ the rate of transfer of any reactants is greatly lower than the chemical change at interface. Combining equations 12 and 13, one obtains:

$$j_i = 0.62 C_{o_i} D^{2/3} \nu^{-1/6} \omega^{1/2}$$

If one multiplies the above equation by a number of electrons participating in the reaction (n) and Faraday's constant (F), the removal rate of copper in the chemical planarization process can be obtained with:

$$i_1 = 0.62 n F C_{o_i} D^{2/3} \nu^{-1/6} \omega^{1/2}$$

Upon examination of this equation, it can be observed that the physical properties of the electrolyte such as viscosity, density, concentration of solute and diffusivity play some role in planarization of copper. The removal current density (or corrosion current density), i_1 shows a linear relationship with the square root of angular speed of rotating electrode ω .

Under static conditions or when rotating speed is very low, the above equation takes the form:

$$i_{pk}/F \propto D^{2/3} \Delta C \text{ where } \Delta C = C_o - C_1$$

In summary, the electrochemical planarization of copper using a disk electrode can be affected by multiple variables such as, the rotating speed, viscosity of the electrolyte, concentration of electrolyte, and the diffusivity of the electrolyte species.

PROPERTIES OF ELECTROPOLISHED SURFACES

The physical, corrosion, and mechanical properties of a polished surface depends on the nature and the surface state of metals electropolished¹³. The main variables consist of physical characteristics (crystalline lattice structure, stresses & strains), chemical nature and surface geometry (distribution of peaks and crevices). Mechanically polished surfaces may have an amorphous or mechanically deformed layer which may influence its oxidation behavior.

However, this layer may gradually transmit back to the crystalline structure following electropolishing pending its thickness. Monitoring of chemical composition using scanning electron microscopy is generally one means to analyze surface heterogeneity and its effect on electropolishing.

EFFECT OF ELECTROPOLISHING ON PROPERTIES OF METALS

Mechanical properties of electropolished metals such hardness, Young's modulus may be improved. In some materials such as stainless steel no change is observed in mechanical properties (static strength parameters)¹³. An effect on fatigue behavior is difficult to determine^{13,19} due to complex nature of failure which involves stress concentration, cracks or surface defects. Generally, mechanical polishing produces a cold-worked surface layer which enhances fatigue life of materials. During electropolishing if this surface is removed, then fatigue life may be reduced. On the contrary, electropolishing can remove surface defects responsible for initiating fatigue cracks which could reduce the fatigue-life. the surface roughness of the metal is reduced by electropolishing which may increase the fatigue life, for instance in steel¹³.

Since the cold-worked layer is removed during electropolishing, magnetic properties of material such as steel may be improved. Surface conductance is also improved for an electropolished surface. The effect of electrolytic polishing on corrosion properties of metals depends on the post polished oxide that forms and how porous the protective film in an acidic or basic solution. General corrosion is generally improved or no difference is observed following polishing¹⁸. In the case aluminum, a protective oxide film is observed and has proven to be beneficial.

CHAPTER 3

EXPERIMENTAL PROCEDURE

Each electrolyte using phosphoric acid containing copper was made prior to each test. For conductivity and viscosity measurements, the total volume of solution was between 64 and 78 milliliters in order to conserve chemicals. A significant number of solutions had to be made in order to determine the effect of copper on higher phosphoric acid concentration for each physical measurement. Since the volume for each concentration varied with the fixed amount of copper added to each solution, the overall concentration of copper in each phosphoric acid solution was different. Each test cell was visually examined to ensure no precipitate is present prior to any test. Part of each electrolyte that was not used for any test was stored for stability evaluation and observed daily for any sign of precipitation.

The sample (anode) for the rotating disk electrode was made of 99.998% pure fully annealed polycrystalline copper. The copper-coated wafer was made from single crystal silicon and consisted of a base silicon wafer covered with a diffusion barrier layer of tantalum approximately 1.5 μm thick and an as-plated top layer of copper that was 1.0, 2.0 or 4 μm in thickness.

PHYSICAL MEASUREMENTS

Conductivity Measurement

Conductivities were performed using a Model ES-12 Horiba conductivity meter. The electrode was placed in the volumetric flask to measure conductivity at temperature from 2 °C to 40 °C. Standard 0.1 N KCl was used to calibrate the electrode. Temperature compensation was set for higher temperature measurements. Conductivity of phosphoric acid having concentrations of 0.3 M to 1.4 M copper were measured. Electrolytes having concentrations above 1.5 M were eliminated from evaluation due to precipitation problems encountered.

Viscosity Measurements

Based on Levich equation, viscosity has a tremendous impact on polishing removal of copper¹⁸. In addition, since the amount of copper in the phosphoric acid solution was increased, it was believed the viscosity would increase with increasing copper. A Brookfield programmable DV II viscometer was used to measure viscosity. The meter was calibrated and then placed into the solution of interest. Most measurements were obtained at 60 rpm at temperatures between 0 °C and 40 °C.

pH Measurements

An Orion Model 250 pH meter, was used to measure pH in all stages of experiments. The initial measurements were taken in conjunction with viscosity tests. The pH electrode was calibrated by buffer solutions of pH 4 and pH 7. Measurements were taken at temperatures between 0 °C and 40 °C.

Density Measurements

Following the completion of the conductivity tests, a 10 milliliter-graduated cylinder was used to weigh the electrolyte and to calculate the density for each solution.

POTENTIODYNAMIC POLARIZATION EXPERIMENTS

All experiments were carried out with copper as the anode in an electrolyte containing 45-85% phosphoric acid with different levels of copper at room temperature (22.5 °C). The electrode was a cylindrical copper disk (99.9% purity) with an area of 0.285 cm². The samples were mechanically polished with abrasive sand paper stepwise from 320 grit to 800 grit followed by cleaning in methanol, acetone, and deionized water and dried with air. A fresh electrolyte was used in each experiment. A corrosion test cell consistent with the ASTM standard G-3 was used to run a series of potentiodynamic tests on the rotating copper disk electrode. Prior to each experiment, all glassware was cleaned with soap and rinsed thoroughly with distilled water, then 55 to 85% ortho-phosphoric acid solutions were employed to determine the effect of acid concentration on the anodic dissolution of copper.

Reported potentials were measured with respect to a saturated calomel electrode (SCE) and have been corrected for the IR drop (Figure 6). A platinum mesh (Johnson Matthey) was used as the counter electrode. Before each experiment, 400 milliliters of the phosphoric solution was poured in the corrosion cell, then both the working electrode and counter electrode were placed in the solution. An EG & G Model 1150 Rotating Disk Electrode was used to introduce the working electrode. Rotation speeds of 25, 50, 100, 200 and 860 rpm were used to determine the hydrodynamic effect of the electrolyte on electropolishing of copper.

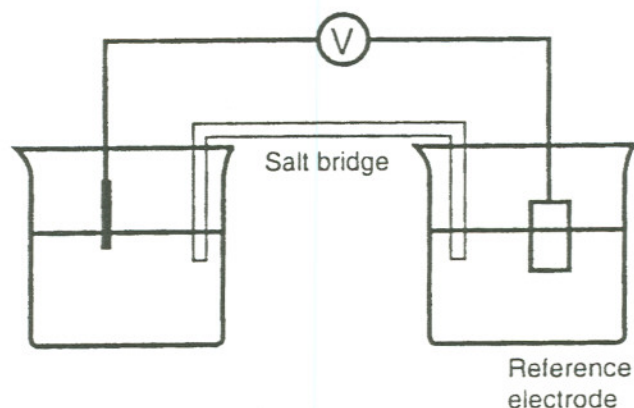


Figure 6. Schematic of a polarization cell³.

The potential and current were measured using an automated EG & G Model 273 potentiostat. Prior to potential scanning, a stable free corrosion potential was obtained. In this test study, a potentiodynamic test method was utilized where a fixed electrochemical potential versus the reference electrode was applied at 10 millivolts per second and the resulting current for each applied potential recorded by the computerized EG & G system. There are various electrochemical plots to show resulting current versus potential such as linear I-V or log I-V. Figure 3 shows an idealized plot of current (density) vs. applied potential as a linear plot for a typical electrolyte. In this figure, line AB represents a metal dissolution where also etching occurs. The main areas for electropolishing region lies along the BE line; however, an ideal polishing region for planarization is in the CD area before any oxygen contamination occurs in the transpassive zone. This behavior is a typical mechanism observed in the anodic dissolution and in the electropolishing of copper in ortho-phosphoric acid.

POTENTIOSTATIC EXPERIMENTS

Constant potentials from passive and transpassive zones were applied in the potentiostatic experiment. The potentials were determined from the polarization curves obtained in each environment. The potentiostatic experiment provides steady state current at the applied potentials from the two regions where the specimen surface was electropolished, i.e., the passive and the transpassive regions. During the experiment, current density with time was monitored. All potentiostatic experiments were carried out for three minutes.

OPTICAL AND SCANNING ELECTRON MICROSCOPY (SEM) EXAMINATION

Prior to and following the potentiodynamic and potentiostatic tests, the wafer samples were examined using the Olympus PM E-3 PMEU optical microscope at Merix, Inc. Wafers used for testing were provided by Novellus Systems, Inc. The wafers were cleaned with distilled water, methanol, acetone, and then dried. Optical pictures were taken using Sony VIA-100 camera RGB and Extron Video imaging tool. While maximum magnification of the system was limited to 1000 X; most of the images were recorded at 100 X or 200 X.

SEM specimens were directly examined using a Hitachi S-350 N SEM linked with an Oxford Energy Dispersive Spectrometry System (EDX) for elemental analysis. Images were recorded using secondary electron and backscattered techniques. The wafers were initially polished to 800 grit prior to cleaning and electrochemical tests performed without any further mechanical polishing. Microstructural analyses were performed using backscattered imaging. X-ray analysis was used to identify the composition of the base materials, oxide layers and any phosphorous compounds after each test.

SURFACE ROUGHNESS MEASUREMENTS

The conditions of the surface following the potentiodynamic and potentiostatic experiments were examined by measuring the surface roughness. A Veeco Detak Model 300Si contact Profilometer was used for these measurements.

CHAPTER 4

RESULTS AND DISCUSSION

PHYSICAL MEASUREMENTS

Stability

Electrolytes with varying concentrations of phosphoric acid and copper oxide appeared to be unstable as they aged. In addition, with higher concentration of copper in Ortho-phosphoric acid, the precipitation of copper byproducts was increased as the electrolyte aged with time. This instability created an extra dimension to the test variables. The precipitation especially increased above a 1.2 M copper level. Based on the test results with 85% phosphoric acid, the maximum copper that could be dissolved in this solution was found to be between 0.75-1.0 M soluble. Copper did not appear to be in the 85% phosphoric acid at room temperature and solubility of copper decreased with increasing acid concentration.

Based on previous studies³, the ideal phosphoric acid concentration for electropolishing copper was found between 60%-70%. Therefore, the electrolyte solutions with 60%, 65% and 75% phosphoric acid and a copper concentration of 0.8 and 1.2 M to obtain maximum electropolishing, to avoid precipitation, and to maintain stable test solutions.

In a prescreening study for physical measurements and solution stability determination, a solution of 45% phosphoric acid with as little as 0.12 M copper was used. The upper boundary for dissolved copper was found at 1.65 M in 75% phosphoric acid and 0.70 M in 85% phosphoric acid. However, these upper threshold levels were only stable for about 24 hours after which precipitation of copper phosphate products quickly resulted.

Conductivity

The conductivity values obtained are shown in Figures 7. through 11. As expected, the highest conductivity values were found for the solutions containing the lowest concentration of copper in phosphoric acid solutions up to 65%. The conductivity of electrolytes of 75% and 85% H_3PO_4 showed lower conductivities than those of 60%-65% H_3PO_4 . The lowest conductivity values were found in solutions with highest concentration of copper ions.

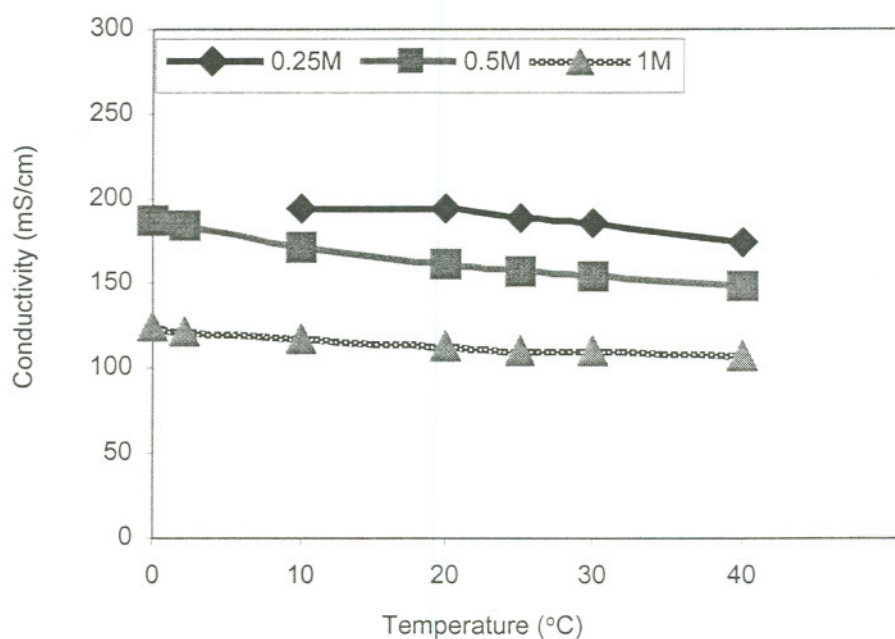


Figure 7. Conductivity measurements vs temperature in 45% H_3PO_4

This dependence is observed at each temperature. As the copper concentration decreased below 0.5M Cu in 45% and 60% H_3PO_4 , the conductivity decreased with increasing temperature except at high concentrations of H_3PO_4 . Above the concentration of about 0.5M Cu^{2+} , the conductivity increased with temperature. This may be associated with forming different complexes between copper and phosphoric acid^[32].

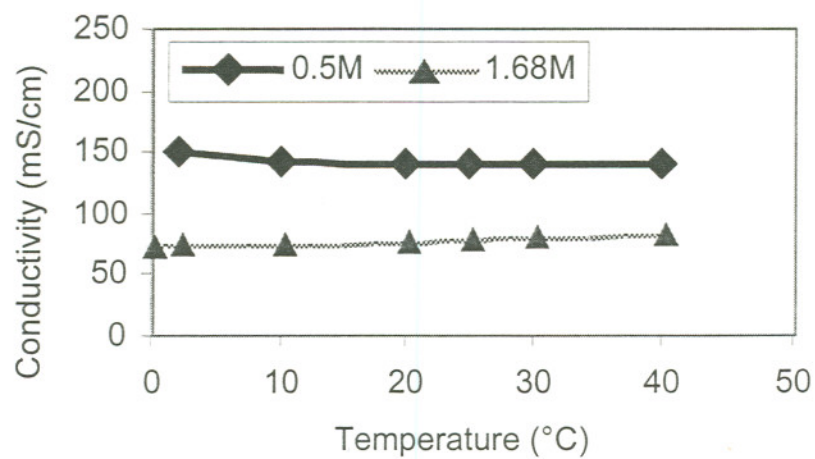


Figure 8. Conductivity measurements vs temperature in 60% H_3PO_4

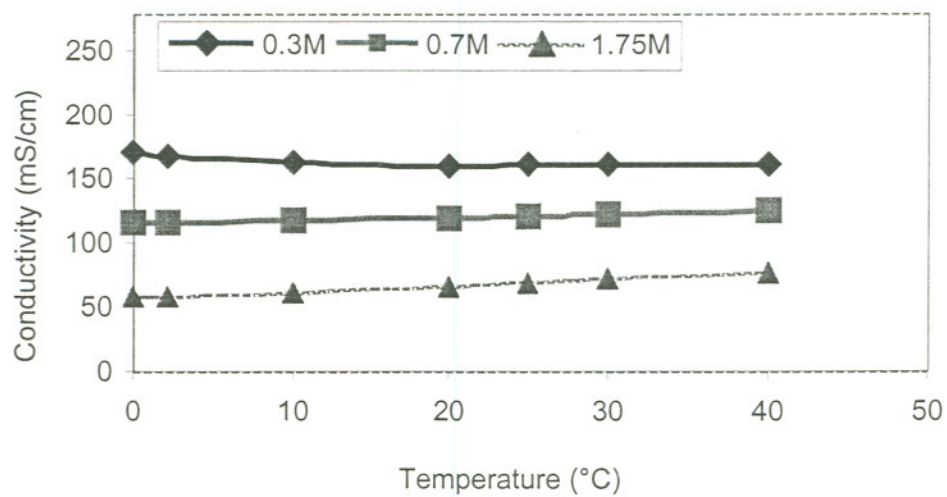


Figure 9. Conductivity measurements vs temperature in 65% H_3PO_4

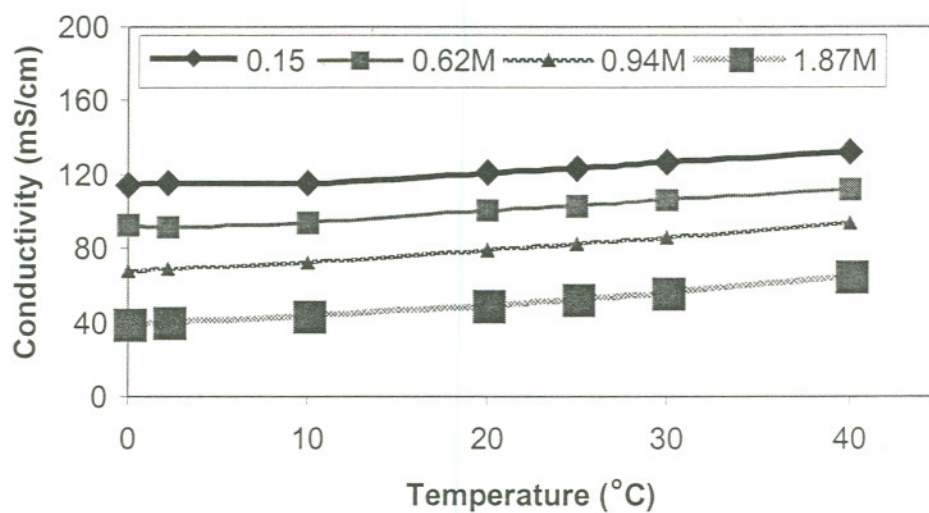


Figure 10. Conductivity measurements vs temperature in 75% H₃PO₄

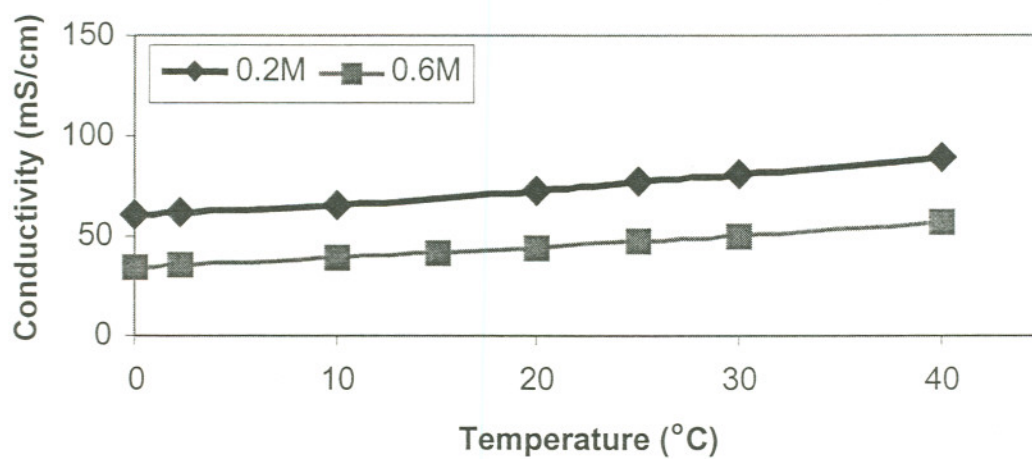


Figure 11. Conductivity measurements vs temperature in 85% H₃PO₄

Viscosity Measurement Results

Generally, dissolved copper raises the viscosity of phosphoric acid and is dependent on amount of copper per unit volume. The higher the concentration of copper in phosphoric acid, the greater the viscosity of the electrolyte¹⁹. Temperature also greatly affects the relative viscosity. Figures 12 through 14 show the viscosity values in 65%, 75% and 85%, H₃PO₄ containing copper ions as a function of temperature. As the temperature increased, the viscosity values of each solution decreased. A decrease in viscosity with increasing temperature could be attributed to higher solubility of copper in the phosphoric acid at lower temperatures.

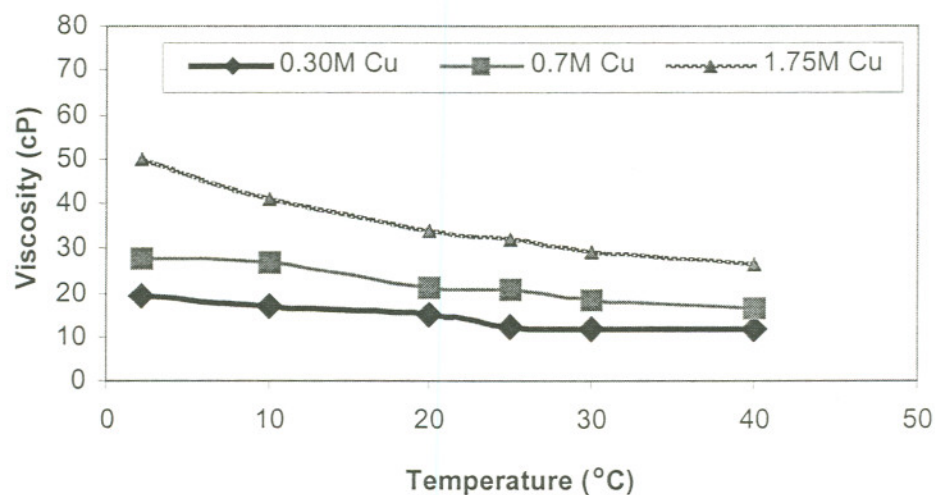


Figure 12. Viscosity measurements vs temperature in 65% H₃PO₄

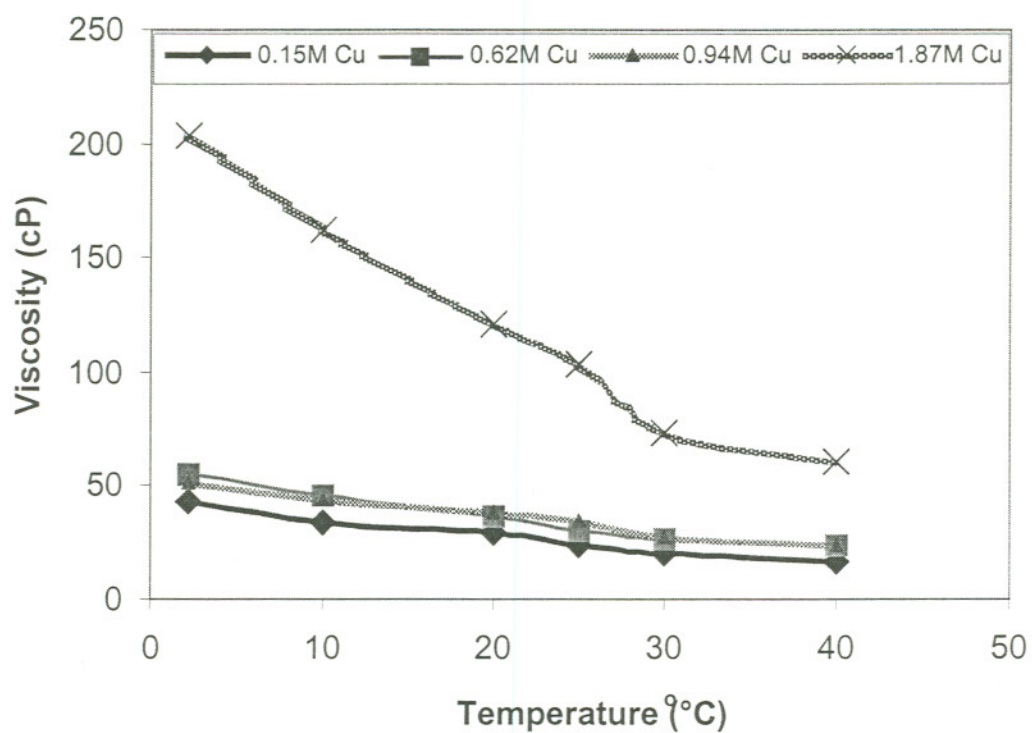


Figure 13. Viscosity measurements vs temperature in 75% H₃PO₄

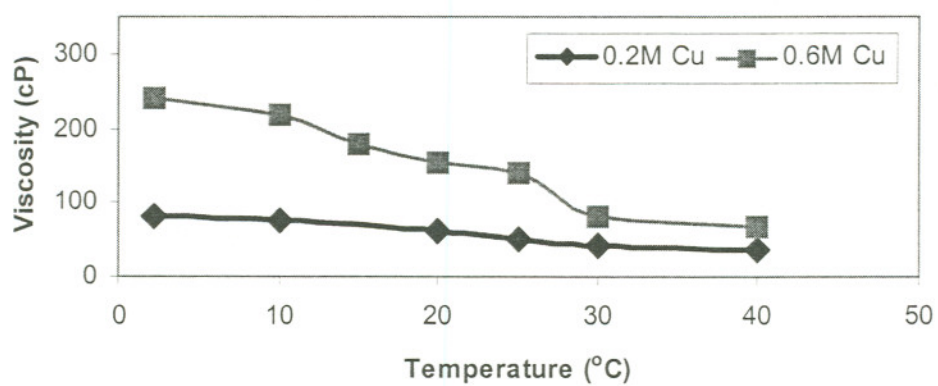


Figure 14. Viscosity measurements vs temperature in 85% H₃PO₄

In the 65% H_3PO_4 and 75% H_3PO_4 (Figure 12 and 13, respectively) electrolytes at any given temperature ($0^\circ - 40^\circ \text{C}$), the viscosity values increased with increasing concentration of copper. In 45% H_3PO_4 and 60% H_3PO_4 , the same viscosity trend was observed up to 30°C and in 65% H_3PO_4 viscosity trend was also similar approximately up to 25°C .

The rate of viscosity change decreased in 75% H_3PO_4 and 1.87M Cu^{2+} between 25°C and 30°C (Figure 13). A similar decay in viscosity value is observed within the same temperature range is observed in 85% H_3PO_4 containing 0.6M Cu^{++} (Figure 14). This decline could be attributed to precipitation of copper phosphate. With the presence of copper phosphate, the viscosity is higher which may affect the diffusivity of phosphoric acid. The solubility limit of copper phosphate in the electrolyte as a function of temperature appears to be the dominant factor in determination of the viscosity of the solution. This hypothesis has also been verified by other authors^{19,23,24}.

As the concentration of H_3PO_4 increases, the sensitivity of the viscosity to Cu^{2+} concentration increases. The rate of change in viscosity with temperature fluctuation increases with increasing H_3PO_4 concentration, and also becomes more sensitive to as H_3PO_4 increases; i.e, small changes in concentration of Cu^{2+} means large fluctuations in viscosity, and large increases in overall rate of viscosity change with temperature fluctuations.

Density Measurement Results

Since solution preparation of electrolyte is a tedious effort of dissolving copper in phosphoric acid, a slight variation of copper concentration may be observed in the overall solution chemistry due to potential fluid evaporation while preparing the electrolyte. The density results were fairly consistent. As shown in Table 2, generally, the densities increased with increasing copper concentration at constant temperatures. Additionally, higher densities were obtained for higher concentration of phosphoric acid. The laboratory density results for 85% phosphoric acid was found at 1.67 g/cm^3 and was very close to the density value 1.69 g/cm^3 provided by the manufacturing company. Overall, the density values decreased from 1.67 g/cm^3 to 1.44 g/cm^3 with a decrease of phosphoric acid concentration from 85% to 45%. The addition of copper increased the density.

pH of the Electrolytes

As discussed in the procedure section, the pH of the each electrolyte was measured at 25°C. The pH values are shown in Tables 2. The results were found to range from 0.2 pH and 0.8 pH, a very narrow range.

Table 2. Density pH measurements of H₃PO₄ and Cu²⁺, Temp = 25 °C.

Electrolyte (H ₃ PO ₄)	Cu (m/l)	Density (g/Cm3)	pH
85%	0.2	1.6814	0
	0.6	1.7936	0
75%	0.1	1.57	0.3
	0.62	1.58	0.4
	0.94	1.61	0.2
	1.87	1.75	0.2
65%	0.2	1.43	0.6
	0.50	–	0.7
	1.20	1.62	0.5
60%	0.56	1.46	0.6
	0.84	1.49	0.5
45%	1.68	1.52	–
	0.25	1.3	0.2
	0.5	1.4	–

Table 3. Slope of Conductivity Plots.

Sample (H ₃ PO ₄)	Cu (M)	m	R ²
85%	0.2	0.72	0.992
	0.6	0.554	0.992
75%	0.15	0.444	0.964
	0.62	0.444	0.963
	0.94	0.636	0.993
	1.87	0.628	0.984
65%	0.30	-0.23	0.718
	0.70	0.255	0.96
	1.75	0.465	0.989
60%	0.20	-0.26	0.697
	0.60	0.23	0.978
50%	0.40	-0.651	0.921
	0.52	-0.052	0.331
	1.00	-0.089	0.86
45%	0.25	-0.65	0.861
	0.50	-0.981	0.955
	1.00	-0.419	0.946

Table 4. Slope of Viscosity Plots.

Sample (H ₃ PO ₄)	Cu (M)	m	R ²
85%	0.2	-1.27	0.957
	0.6	-5	0.978
75%	0.15	-0.688	0.97
	0.62	-0.872	0.957
	0.94	-0.731	0.972
	1.87	-3.91	0.97
65%	0.30	-0.215	0.897
	0.70	-0.33	0.962
	1.75	-0.62	0.942
60%	0.20	0.018	0.0263
	0.60	-0.512	0.983
50%	0.40	-0.143	0.956
	0.52	-0.089	0.86
	1.00	-0.118	0.966
45%	0.25	-0.13	0.994
	0.50	-0.042	0.9041
	1.00	-0.04	0.889

Table 5. Physical Measurements.

Variable	Conductivity		Comments
Cu ⁺⁺	↓	↑	Up to 65% H ₃ PO ₄
H ₃ PO ₄	↑	↓	
T (°C)	↑	↓	Up to 75% H ₃ PO ₄
Viscosity			
Cu ⁺⁺	↑	↑	
H ₃ PO ₄	↑	↑	
T (°C)	↑	↑	Except 45% & 65% H ₃ PO ₄ >40 °C
Density			
Cu ⁺⁺	↑	↑	
H ₃ PO ₄	↑	↑	

Table 6. Conductivity and Viscosity Measurements of Electrolytes containing 45% H_3PO_4 with 0.25 M Cu as a function of temperature.

Temp (°C)	Conductivity mS/cm	Viscosity cP
0	–	–
2.2	–	6.8
10	194	6.53
20	194	5.84
25	189	6.18
30	186	5.49
40	175	5.32

Table 7. Conductivity and Viscosity Measurements of Electrolytes containing 45% H_3PO_4 with 0.5M Cu as a function of temperature.

Temp (°C)	Conductivity mS/cm	Viscosity cP
0	187	–
2.2	184	8.53
10	171	8.74
20	161	8.15
25	157	7.75
30	154	7.46
40	149	7.17

Table 8. Conductivity and Viscosity Measurements of Electrolytes containing 45% H_3PO_4 with 0.76M Cu as a function of temperature.

Temp (°C)	Conductivity mS/cm	Viscosity cP
0	153	–
2.2	150	11.1
10	141.2	9.8
20	134.3	8.6
25	132	7.9
30	130.2	7.51
40	126.7	6.99

Table 9. Conductivity and Viscosity Measurements of Electrolytes containing 45% H_3PO_4 with 1M Cu as a function of temperature.

Temp (°C)	Conductivity mS/cm	Viscosity cP
0	124.2	–
2.2	121.5	11.4
10	117	10.6
20	112.4	9.13
25	110.4	8.73
30	109.4	7.75
40	107.5	6.47

Table 10. Conductivity and Viscosity Measurements of Electrolytes containing 50% H_3PO_4 with 0.395M Cu as a function of temperature.

Temp (°C)	Conductivity mS/cm	Viscosity cP
0	181.8	–
2.2	178.8	9.42
10	167.5	8.9
20	161.2	7.92
25	158.9	7.4
30	156.6	6.5
40	153	4.91

Table 11. Conductivity and Viscosity Measurements of Electrolytes containing 50% H_3PO_4 with 0.52M Cu as a function of temperature.

Temp (°C)	Conductivity mS/cm	Viscosity cP
0	164.5	–
2.2	161.1	12.6
10	154.8	11
20	151	9.88
25	149.8	10
30	149.1	9.13
40	141.1	9.19

Table 12. Conductivity Measurements of Electrolytes containing 50% H_3PO_4 with 0.65M Cu as a function of temperature.

Temp (°C)	Conductivity mS/cm
0	154.4
2.2	156.8
10	150.1
20	145.2
25	143.4
30	142.6
40	140.9

Table 13. Conductivity and Viscosity Measurements of Electrolytes containing 50% H_3PO_4 with 1.05M Cu as a function of temperature.

Temp (°C)	Conductivity mS/cm	Viscosity cP
0	111.6	–
2.2	110.4	16.2
10	108.2	13.8
20	107.9	13.1
25	108.2	12.4
30	108.7	11.5
40	109.2	10.4

Table 14. Conductivity and Viscosity Measurements of Electrolytes containing 50% H_3PO_4 with 1.57M Cu as a function of temperature.

Temp (°C)	Conductivity mS/cm	Viscosity cP
0	73.5	–
2.2	73.9	27.5
10	74.9	24.4
20	76.8	20.1
25	77.9	18.7
30	78.9	16.7
40	80.9	16

Table 15. Conductivity Measurements of Electrolytes containing 50% H_3PO_4 with 2.63M Cu as a function of temperature.

Temp (°C)	Conductivity mS/cm
0	35.3
2.2	35.5
10	37.4
20	40.1
25	41.3
30	42.8
40	46

Table 16. Conductivity and Viscosity Measurements of Electrolytes containing 60% H_3PO_4 with 0.56M Cu as a function of temperature.

Temp (°C)	Conductivity mS/cm	Viscosity cP
0	147.7	–
2.2	146.9	19.1
10	143.8	18
20	142.8	17.1
25	143.2	15.5
30	143.8	15.1
40	144.9	15

Table 17. Conductivity and Viscosity Measurements of Electrolytes containing 60% H_3PO_4 with 0.7M Cu as a function of temperature.

Temp (°C)	Conductivity mS/cm	Viscosity cP
0	148.3	–
2.2	150.2	19.7
10	142.6	22.3
20	140.3	23.5
25	139.3	23.2
30	139.4	22.2
40	139.3	20.5

Table 18. Conductivity and Viscosity Measurements of Electrolytes containing 60% H₃PO₄ with 0.7M Cu as a function of temperature.

Temp (°C)	Conductivity mS/cm	Viscosity cP
0	148.3	–
2.2	150.2	16.1
10	142.6	14.6
20	140.3	13.1
25	139.7	12.5
30	139.4	11
40	139.3	9.8

Table 19. Conductivity and Viscosity Measurements of Electrolytes containing 60% H₃PO₄ with 0.84M Cu as a function of temperature.

Temp (°C)	Conductivity mS/cm	Viscosity cP
0	118.7	–
2.2	117.6	31.2
10	115.5	25.4
20	117.2	20.8
25	118.8	18.7
30	120.4	15.5
40	123.4	14.6

Table 20. Conductivity and Viscosity Measurements of Electrolytes containing 60% H₃PO₄ with 1.686M Cu as a function of temperature.

Temp (°C)	Conductivity mS/cm	Viscosity cP
0	71.5	–
2.2	72.6	36.6
10	73	33.1
20	75.4	28.5
25	76.9	24.6
30	78.3	21
40	81	18.3

Table 21. Conductivity and Viscosity Measurements of Electrolytes containing 60% H_3PO_4 with 0.84M Cu as a function of temperature.

Temp (°C)	Conductivity mS/cm	Viscosity cP
0	129.3	–
2.2	127.8	23.1
10	124.7	19.1
20	125.2	18.3
25	126.2	16.9
30	127	14.7
40	128.7	14.8

Table 22. Conductivity and Viscosity Measurements of Electrolytes containing 65% H_3PO_4 with 0.29M Cu as a function of temperature.

Temp (°C)	Conductivity mS/cm	Viscosity cP
0	170	–
2.2	168	19.1
10	162.4	17
20	160.3	14.9
25	160.4	12.1
30	160.5	11.8
40	160.5	11.7

Table 23. Conductivity and Viscosity Measurements of Electrolytes containing 65% H_3PO_4 with 0.73M Cu as a function of temperature.

Temp (°C)	Conductivity mS/cm	Viscosity cP
0	115.3	–
2.2	115.5	28
10	116.8	26.8
20	118.6	21
25	120.6	20.7
30	122.1	18.5
40	125.8	16.4

Table 24. Conductivity and Viscosity Measurements of Electrolytes containing 65% H_3PO_4 with 1.74M Cu as a function of temperature.

Temp (°C)	Conductivity mS/cm	Viscosity cP
0	58.2	—
2.2	58.3	50.1
10	61.1	41.1
20	65.6	34.1
25	68.6	31.9
30	71.3	29
40	76.5	26.2

Table 25. Conductivity and Viscosity Measurements of Electrolytes containing 70% H_3PO_4 with 1.5M Cu as a function of temperature.

Temp (°C)	Conductivity mS/cm	Viscosity cP
0	53	62.5
2.2	53.2	62.6
10	57.5	65.1
20	64.6	55.1
25	66.6	49.5
30	69.1	47.9
40	75.4	42.3

Table 26. Conductivity and Viscosity Measurements of Electrolytes containing 75% H_3PO_4 with 0.15M Cu as a function of temperature.

Temp (°C)	Conductivity mS/cm	Viscosity cP
0	114.2	
2.2	114.8	42.6
10	115.7	34.2
20	120.5	29
25	123.3	23.8
30	126.1	20.1
40	132.2	16.9

Table 27. Conductivity and Viscosity Measurements of Electrolytes containing 75% H_3PO_4 with 0.62M Cu as a function of temperature.

Temp (°C)	Conductivity mS/cm	Viscosity cP
0	92.2	
2.2	91.8	55
10	94.1	46
20	100.1	36.6
25	103.2	30.2
30	105.9	26.3
40	112.3	23.6

Table 28. Conductivity and Viscosity Measurements of Electrolytes containing 75% H_3PO_4 with 0.78M Cu as a function of temperature.

Temp (°C)	Conductivity mS/cm	Viscosity cP
0	77.9	—
2.2	78.1	55.7
10	81.5	43.5
20	87.5	40.7
25	91	35.8
30	94.4	31.7
40	101	26.7

Table 29. Conductivity and Viscosity Measurements of Electrolytes containing 75% H_3PO_4 with 0.94M Cu as a function of temperature.

Temp (°C)	Conductivity mS/cm	Viscosity cP
0	68.2	—
2.2	68.6	51
10	72.7	43.5
20	78.9	38.6
25	82.8	35
30	86.4	27.2
40	93.3	23.8

Table 30. Conductivity and Viscosity Measurements of Electrolytes containing 75% H_3PO_4 with 1.25M Cu as a function of temperature.

Temp (°C)	Conductivity mS/cm	Viscosity cP
0	59.3	
2.2	60	65.6
10	63.7	47
20	70.3	43.8
25	73.4	40.3
30	76.8	35.2
40	82.9	29.2

Table 31. Conductivity and Viscosity Measurements of Electrolytes containing 75% H_3PO_4 with 1.87M Cu as a function of temperature.

Temp (°C)	Conductivity mS/cm	Viscosity cP
0	39.6	
2.2	40.3	203
10	44.3	162.4
20	49.8	121
25	53.4	103.5
30	56.5	73.2
40	65.5	60

Table 32. Conductivity and Viscosity Measurements of Electrolytes containing 85% H_3PO_4 with 0.2M Cu as a function of temperature.

Temp (°C)	Conductivity mS/cm	Viscosity cP
0	60.8	
2.2	61.4	81.3
10	65.6	75
20	72.9	60.8
25	77.2	51.2
30	81.5	43.2
40	89.4	36.7

Table 33. Conductivity and Viscosity Measurements of Electrolytes containing 85% H₃PO₄ with 0.6M Cu as a function of temperature.

Temp (°C)	Conductivity mS/cm	Viscosity cP
0	34.6	
2.2	35.5	241.3
10	38.8	219
15	41.9	180
20	44.3	154.3
25	47.1	140.5
30	50.2	80
40	57.1	68

ELECTROCHEMICAL RESULTS

Potentiodynamic Polarization Results

The results of the potentiodynamic experiments shown as anodic polarization curves, are shown in Figures 15 through 18. As previously shown in Figure 3, a plot of current density (A/cm²) versus applied potential (Volts) identifies the areas of interest such as the active region (dissolution of metal), a passivity region, electropolishing, and the oxygen evolution region. Polarization beyond the plateau causes gas evolution as a result of anodic oxidation of water. The potentiodynamic type of plot was used for the experimental determination of electropolishing potential values of copper and to screen electrolytes to find those of interest. A critical step was to determine the ideal potential region to obtain a uniformly planarize surface. The other major task, besides the determination of applied potential, was the identification of ideal electrolytes that must be stable throughout the polishing procedure. Potentiodynamic polarization was used in conjunction with potentiostatic and surface analysis data to determine the ideal planarization current.

The anodic polarization curves indicate the effects of three variables: 1) acid concentration; 2) dissolved copper concentration in the phosphoric acid; and 3) effect of rotating speed which has a hydrodynamic influence on electropolishing of copper in phosphoric acid.

The electrolytic polishing of copper in phosphoric acid was due to the presence of viscous layer $\text{CuHPO}_4 \cdot \text{H}_2\text{O}$ (copper phosphate) at the anode. This viscous layer at the anode controls the rate of dissolution of the product of anodic dissolution, copper phosphate. The mechanism and chemical reactions during electrolytic polishing was outlined in electropolishing of copper in phosphoric acid section. Basically, the polishing current density or planarization current is determined by diffusion rate of metal ions from copper electrode to the solution electrolyte. Since viscous layer is present on the surface of copper, rate of ionization and electrochemical reaction will depend on passage and breakdown of the this viscous layer. The viscous layer is an unstable product and may be detectible using SEM since the product is transitional and may turn into copper phosphate or copper oxide. Copper phosphate can diffuse away from a thin film diffusion layer, especially when the concentration gradient is high.

Effect of Phosphoric Acid Concentration

Figures 15 shows the anodic polarization for copper in 60%, 65% and 75% H_3PO_4 and 0.7M Cu^{2+} at 9 RPM. Copper shows active, active-passive, passive and transpassive behavior.

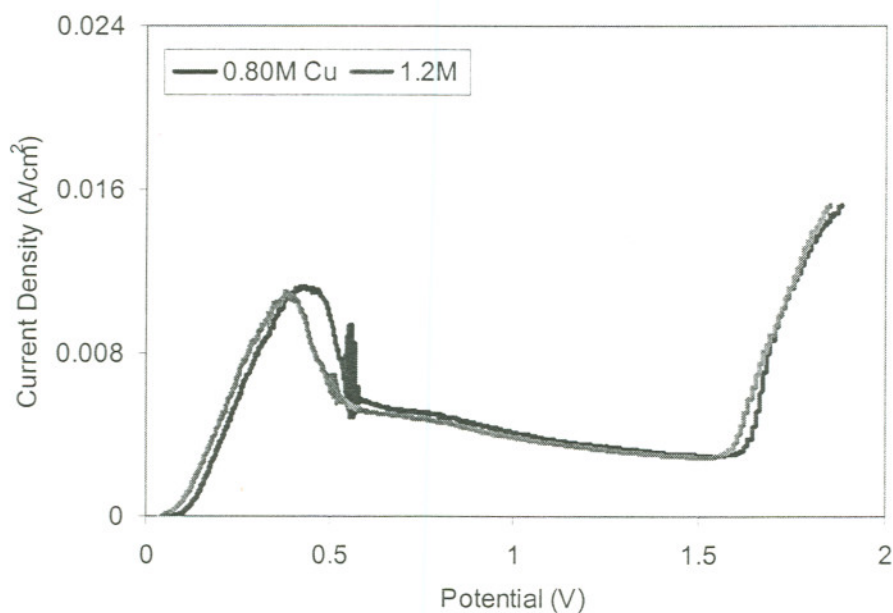


Figure 15. Anodic polarization of copper disk electrode rotated at 9 rpm in 60%, 65%, 75% H_3PO_4 at a copper concentration of 1.2 M Cu^{2+}

A decrease in concentration of phosphoric acid had little or no effect on the value of E_{circuit} , although the polishing current increased significantly. This was also found by previous studies^[19,20], where the maximum polishing occurs at with 20% H_3PO_4 with 3.0M Cu^{2+} . The highest current at any applied potential value was found for copper in 60% phosphoric acid and the lowest in 75% H_3PO_4 . Although the 75% H_3PO_4 appears to be more aggressive than the lower H_3PO_4 concentrations, the potentiodynamic results do not support this observation. This discrepancy could be explained by lower conductivity values for 75% H_3PO_4 with 1.2 Cu^{2+} and with 65% H_3PO_4 , 1.2M Cu^{2+} , as shown in Figures 7 through 11.

Effect of Dissolved Copper

Figure 16 shows the anodic polarization curve for copper in 65% H_3PO_4 containing 0.8 M, and 1.2 M Cu^{2+} . The shape of the polarization curve are similar to each another, regardless of acid and Cu^{2+} concentration. Copper in these electrolytes show active active-passive and transpassive regions. Higher dissolved copper concentration (0.8M vs 1.2M) did not alter current density values significantly for nearly all acid concentration of interest (60%-75%).

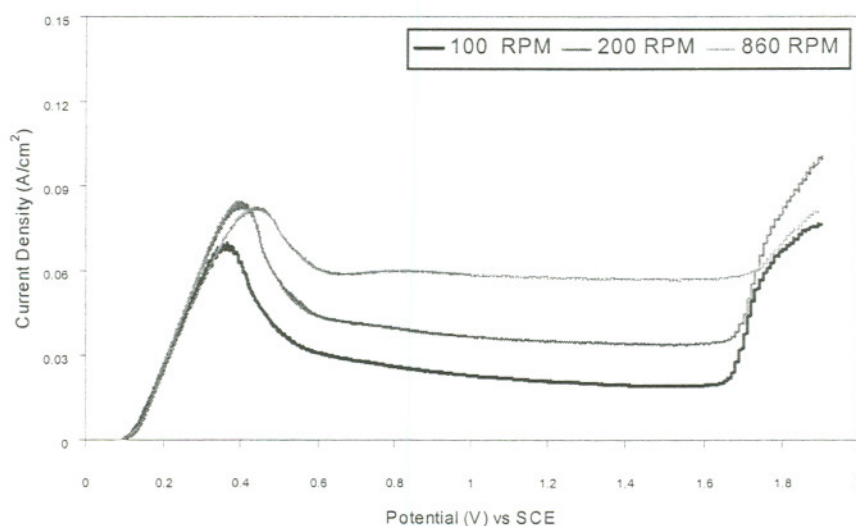


Figure 16. Anodic polarization of wafer coated with thin copper film in 65% H_3PO_4 , rotated at 9 RPM with 0.8 M and 1.2 M Cu^{2+}

Effect of RPM

The hydrodynamic effect of increasing rotation speed is the effective reduction in diffusion or boundary layer thickness. Higher current values for copper in the passive and transpassive regions were observed at higher rotating speed. Figure 16 shows this dependence in 75% of H_3PO_4 containing 1.2 M Cu^{2+} . As can be observed in Figure 17, the current values in the active region do not depend on the RPM values. This indicates that the passivation process is controlled by concentration polarization (diffusion / mass transport) whereas the dissolution process is controlled by activation polarization^{20,22}.

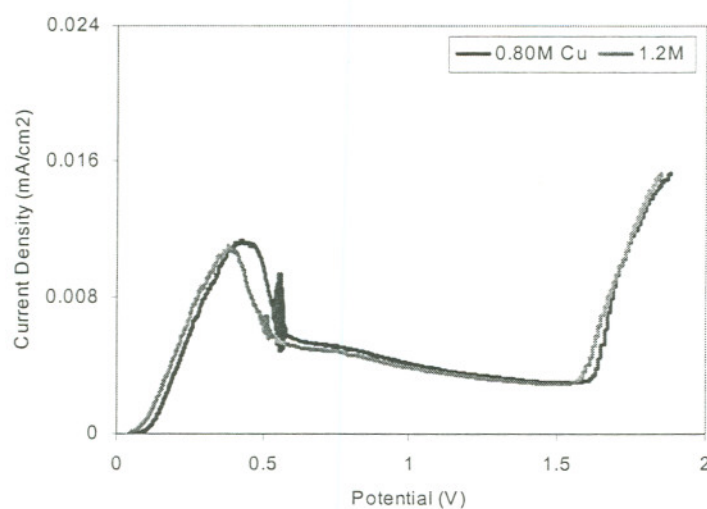


Figure 17. Anodic polarization of copper disk electrode rotated at 100, 200, and 300 rpm in 75% H_3PO_4 and 1.2 M Cu^{2+}

Based on the previous studies^[31], the optimum metallographic electropolishing could be obtained in solutions containing 60-70% (8.7-10 M) ortho-phosphoric acid at temperatures between 15-25 °C. The brightening or electropolishing begins at 36% (5.3M) phosphoric acid^{22,23}.

Effect of Scan Rate

Figure 18 shows the anodic polarization curves of wafers coated with copper at potentiostat scan rates of 10 and 20 mv/sec. The wafer tested at a higher scan rate showed higher removal rate. This confirms that the corrosion process in the passive region is under diffusion control.

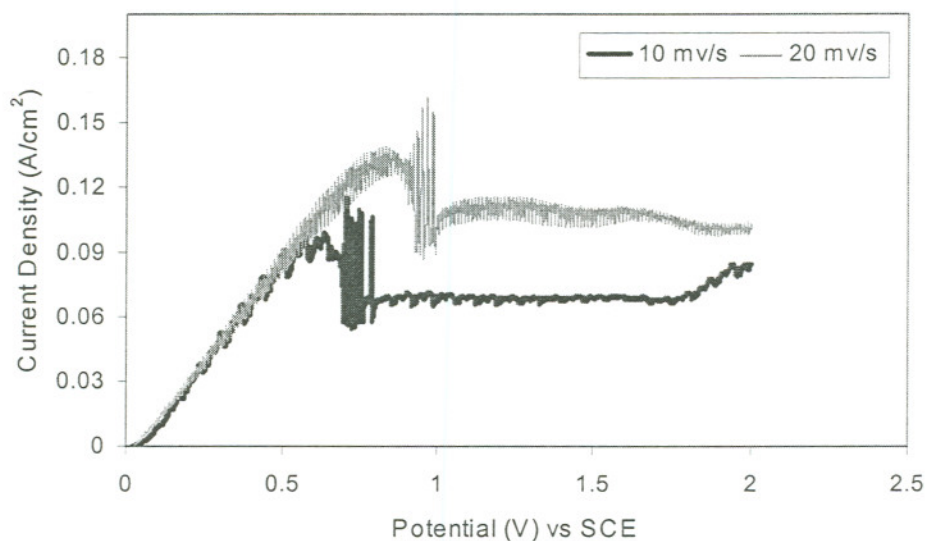


Figure 18. Anodic polarization curves of copper in 65% H_3PO_4 and with 1.2M Cu^{2+} , 10 mv/s and 20 mv/s

POTENTIOSTATIC POLARIZATION RESULTS

The potentiostatic results of the copper disk electrode and the thin film of copper are shown in Figures 19 and 20. Figure 19 shows a plot of current density versus time a mixture of 65% H_3PO_4 with 1.2M Cu^{2+} . The potentiostatic results are divided into a linear and a curved part. The linear part represents the process of dissolution passivation, where the specimen is being passivated. The curved portion represents the process of passivation at the applied potential where the steady state current is achieved.

The I-t curves generated at different rotation speeds values are shown in Figure 20. The results in Figure 20 show the current values increased with increasing rotation speed confirming the reaction is under diffusion control and verifying the potentiodynamic results statement on hydrodynamics as rpm increases. The potentiostatic results are affected by the change in an ion concentration in the surface film or at the solution passive film interface, Also, the results are greatly affected by variation in surface roughness due to perturbation of hydrodynamic boundary layer that affects the dissolution rate.

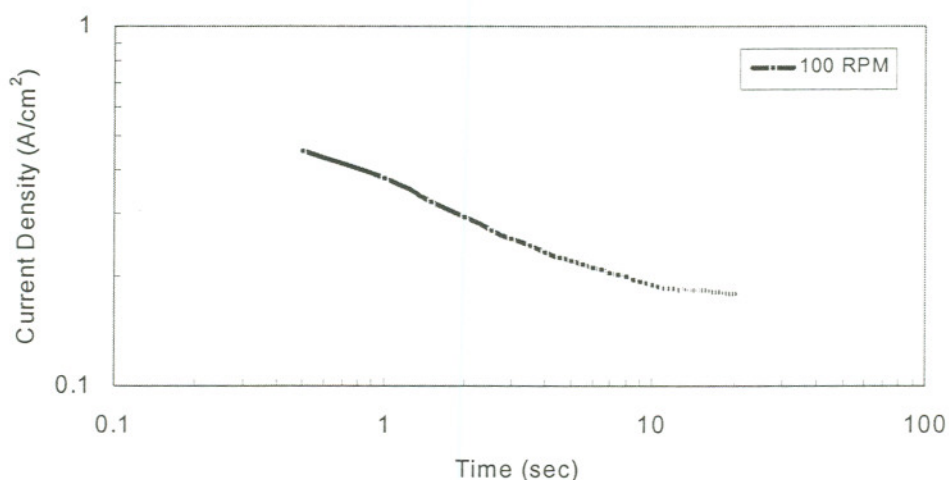


Figure 19. Potentiostatic polarizarion of wafer in 65% H_3PO_4 with 1.2M Cu^{++} , E_{app}

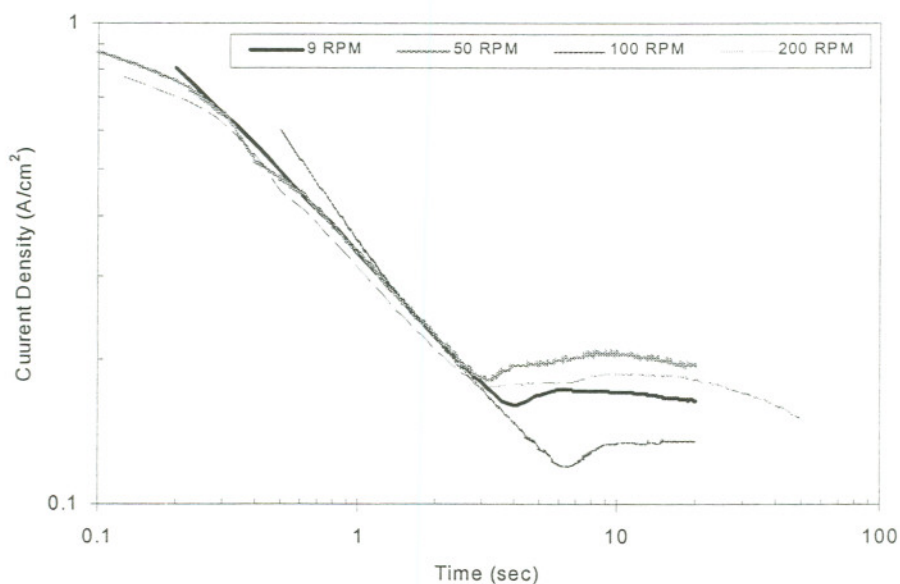


Figure 20. Potentiostatic polarizarion of copper in 65% H_3PO_4 and 1.2M Cu^{++} E_{app}

Table 34. Potentiodynamic Summary

Variable	Planarization	Comments
Cu ⁺⁺	↑ →	No significant Change Min Required 30% H3PO4
H3PO4	↑ ↓	
T (°C)	↑ ↑	
RPM	↑ ↑	
Scan Rate	↑ ↑	

Table 35. Potentiostatic Summary

(Volts)	Planarization
<1.8	Local
1.8	Localized Pitting
2	Uniform Removal
2.2	Uniform Removal
2.4	Severe Pitting

Surface Analysis Results and Discussion

SEM micrographs of the wafer surface before and after the potentiostatic experiments are shown in Figures 21 and 25. The surface roughness measurements for the specimens before and after the 2.0V and 2.2V potentiostatic experiments are shown in Figures 26 and 27, respectively. The SEM photomicrographs obtained for the specimens after the potentiostatic experiments performed at 2.0V and 2.2V showed that uniform removal occurred over the entire surface. Figure 25 shows the results for 2.2V and 2.4V. At the potentials of 1.8V and 2.4V potentiostatic experiments, localized corrosion were observed, and the non-uniformity was reflected in the surface roughness measurements. The surface morphology of the wafer after the potentiodynamic experiment scanned up to 2.2V showed uniform removal of copper (Figure 24).

The EDX results for the wafers before and after the potentiostatic experiments are shown in Figures 21 and 22, respectively. The results indicate that only copper as a metal was present on the wafer surface after the potentiostatic experiment at 1.8V and 2.2V. After the potentiostatic experiment at 2.4V, tantalum was found on the surface of the wafer. A thin tantalum layer had been applied between the silicon wafer and copper surface layer. This indicates the applied potential of 2.4V resulted in excessive removal of copper.

Upon examining the surfaces of the copper electrode and the wafers coated with copper after the potentiostatic tests in the electropolishing region, a white viscous film was observed. The film was presumed to be a copper-phosphorous compound similar that found in the previous studies concerned with electropolishing of copper^{23,24}. This viscous film appeared to be water-soluble and was easily removed by water. SEM examinations of the copper wafer (base), shown in Figure 21, revealed only the presence of copper and oxygen, no phosphorous was detected. No solid film was observed on the surface of electrodes; although, a thin film of Cu_2O was observed on the surface, which is consistent with the previous findings^{20,23,23,25}.

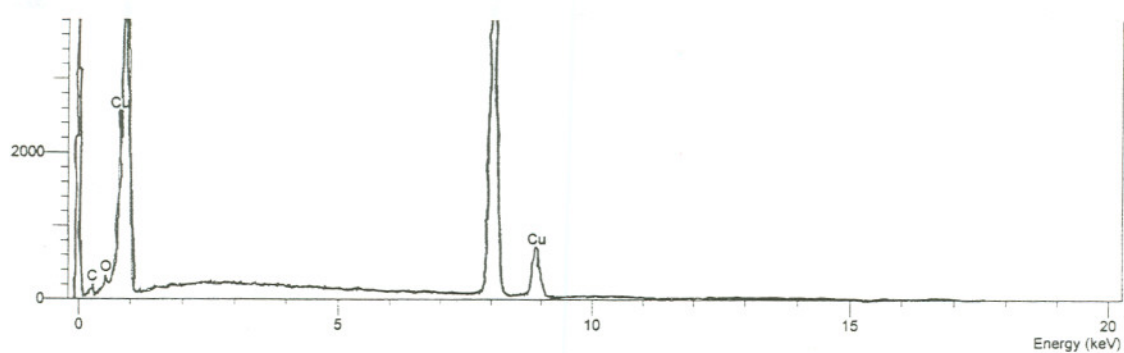


Figure 21. EDX results of the base wafer coated with copper

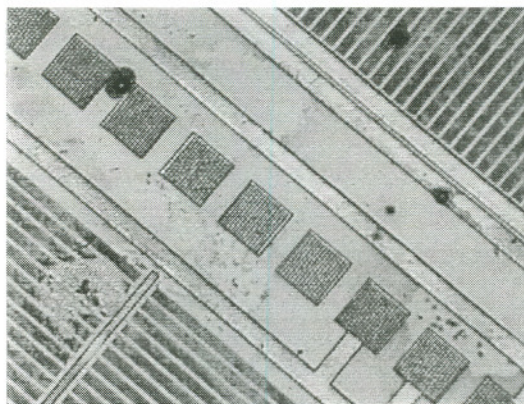
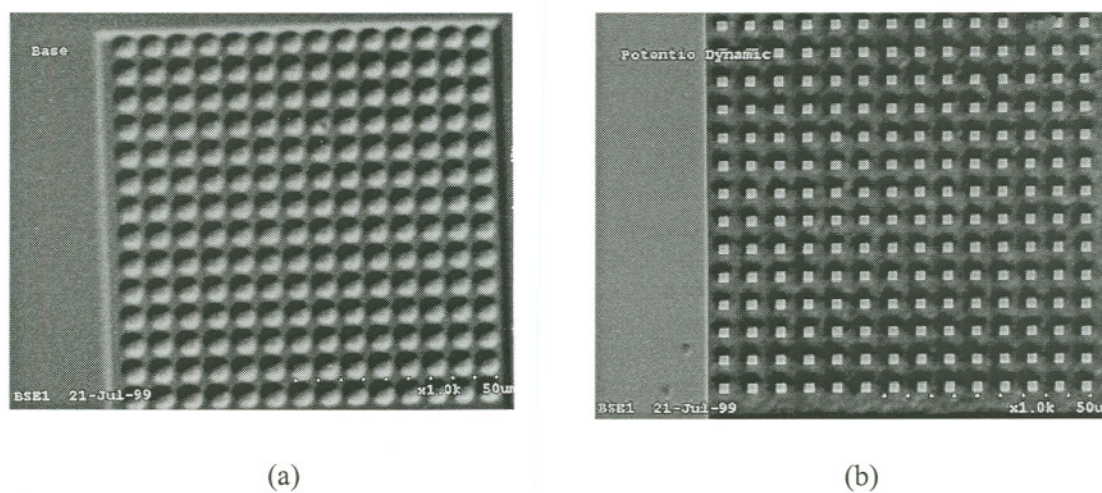


Figure 23. Optical micrograph of base wafer 200x



(a) (b)
Figure 24. SEM micrograph of a wafer 1000x (a) base, (b) following potentiodynamic test.

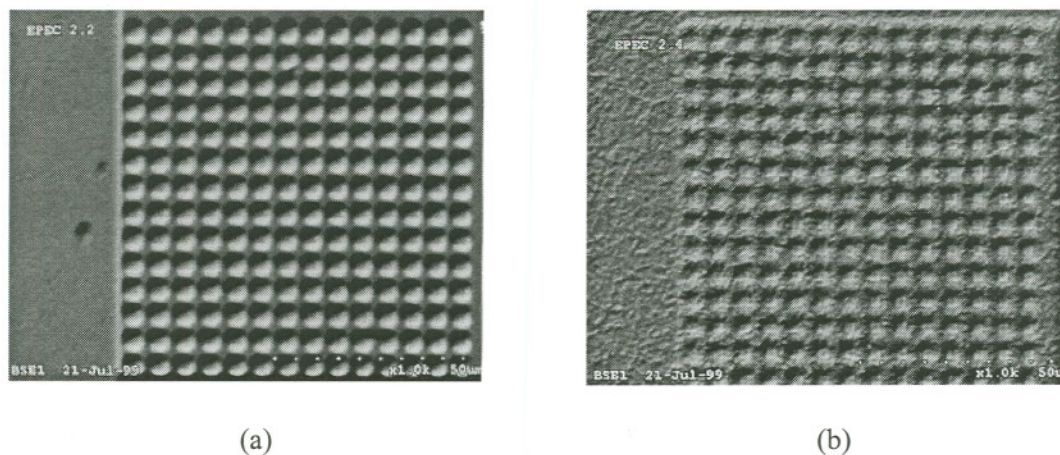


Figure 25. SEM micrograph of a wafer 1500 following potentiostatic test (a) 2.2V, (b) 2.4V

It appears that the potential range of polishing (“Plateau” line CD) in Figure 3 is slightly affected by the dilution of phosphoric acid, but the current rises by increasing the water content or lowering the phosphoric acid concentration. The oxygen evolution potential is also considerably affected by the addition of water. Thus, there is real depolarization of oxygen associated with an increase in water content. Polishing also happens in the transpassive zone, but oxygen levels generated in this potential range may disturb the diffusion layer and make the surface irregular, after certain potential value are applied from the transpassive zone. Figure 15 shows the actual polarization results from various concentrations of phosphoric acid and clearly indicates that lower concentration electrolyte of H_3PO_4 results in higher current densities. This effect is more pronounced in the transpassive region where oxygen evolution occurs.

Also, it is evident that there is a considerable correlation between the polarization curves and the surface features found after electropolishing. In higher acid concentration solutions, it is evident that there is a tendency for breakdown of surface oxide films which contributes to polishing. This effect is more pronounced in the dissolution zone or early stages of electropolishing. The amount of free water present in a surface oxide can influence current density, and therefore, influence the polishing results. Electrolytes with higher water content show higher current densities due to an increased transport through the diffusion layer in the electrolyte.

The formation of pits is associated with decreased polarization of oxygen evolution^{20,24,25}. This perhaps favors streams of oxygen bubbles to be evolved from favorite sites; however, oxygen at higher overpotentials would lead to more uniform and random gas evolution. This is true up to a certain potential value and beyond that potential, the oxygen level increases significantly and pitting is dominant. This is consistent with classical active-passive theory in corrosion studies^{18,24}. The influence of gas evolution on surface finish was considered by Neufeld and Souththal.^(21,22) They suggest that higher degree of polarization of the oxygen evolution reaction would lead to finer, more uniform gassing and would reduce the incidence of surface defects such as pitting and crevices. The mechanisms of gas evolution clearly plays a significant role on surface homogeneity, where higher currents at the edges of a surface may lead to better polishing and results are evident in the potentiostatic results shown in the SEM micrographs at 2.0 and 2.2V vs SCE. However, due to the lack of gas evolution at 1.8V vs SCE, pits formation is possible due to lack of surface inhomogeneity.

Formation of large pits appear on conditions of depolarization of oxygen evolution reaction, where increased gas formation occur in favorite sites and is identifiable to the polarization curves. This effect is shown after potentiostatic test at 2.4V vs. SCE. Not only, the pits appear large but the number of pits increases significantly.

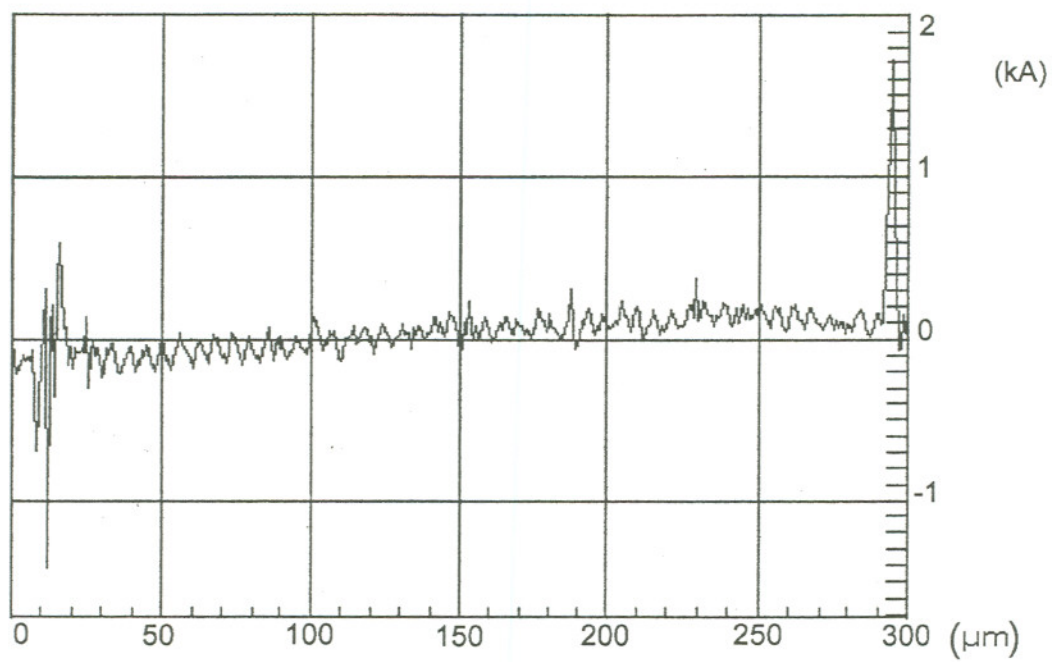


Figure 26. Surface roughness data after potentiostatic tests at 2.0V

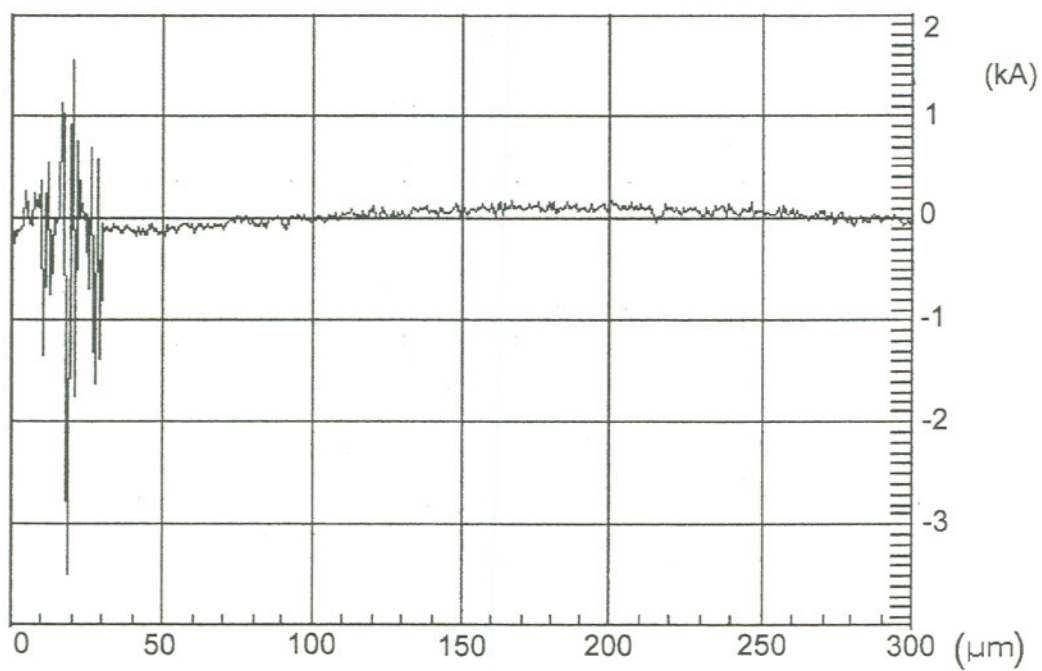


Figure 27. Surface roughness data after potentiostatic tests at 2.2V

CHAPTER 5

CONCLUSIONS

1. The results of the potentiodynamic experiments performed in H_3PO_4 and Cu^{2+} for copper and copper thin film show that copper exhibits active, active-passive, passive and transpassive behavior.
2. The electrochemical results show that current values decreased with decreasing RPM, at any applied potential in the passive and transpassive region. This indicates that these processes are controlled by concentration polarization.
3. The anodic polarization experiment performed as a function of RPM and scan rate of copper in H_3PO_4 and Cu^{2+} show that dissolution of copper in the active region is controlled by activation polarization whereas the passivation process is under concentration polarization (diffusion / mass transport).
4. Current densities increase with decreasing concentration of phosphoric acid indicating higher polishing rates in the solution with lower concentration increased.
5. Based on the potentiodynamic results, a mixture of 60% H_3PO_4 and 1.2M Cu^{++} provides the highest removal rate of copper in the passive and transpassive regions. Also, a high value of conductivity determined for this electrolyte may explain the highest copper removal rate.

6. The surface analysis data show that the applied potentials of 1.8V passive region and 2.4V transpassive region resulted in formation of corrosion pits. The best planarization potentials were found between 2.0V and 2.2V resulting in uniform copper removal. The potentiodynamic curves also supported the potentiostatic results and confirmed uniform removal of copper for planarization applications up to 2.2V without introducing localized corrosion.
7. The electrochemical and surface analysis results indicate that H_3PO_4 containing Cu^{2+} ions could be a suitable solution for electrochemical planarization of copper.

Future Work

In this investigation, an electropolishing technique was used as a new method for planarization. Follow up studies should consist of in-depth investigation of the copper electrode using Transmission Electron Microscopy (TEM) in order to clarify the effect of crystallography and the role of diffusion viscous layer on planarization. In addition, it would be beneficial to compare the results of planarization with wafers that are processed using chemical mechanical polishing method. Since electrolyte plays a significant role in planarization of copper, addition of new compounds beside copper oxide or development of new electrolytes should be studied for comparison purposes. Finally, CMP provides an ideal surface finish required for chip manufacturing. If electropolishing is adopted as a commercial technique, a post surface finish polishing method should be investigated for surface quality issues.

REFERENCES

1. J. W. Mayer, S. S. Lau, *Electronic Materials Science for Integrated Circuits in Si and GaAs*, Macmillan, (1990), p.17.
2. R. Venkatramain, A. Jain., J. Farkas, et al., The Role of the Slurry in the Development of a Copper CMP Process that supports Multilevel, Dual Inlaid Metallization in Semiconductor Devices, *Advanced Interconnects and Contact Materials and Processes for Future Integrated Circuits*. (Materials Research Society Symposium Proceedings, Vol. 514.) Materials Research Society (1998), p. 41-52.
3. J. M. Steingerwald, S. P. Murarka, R. J. Gutmann, *Chemical Mechanical Planarization of Microelectronic Materials*, John Wiley & Sons, Inc., (1997), p.4-10; 19-33; 42-47; 90-124.
4. M. B. Beaver, *Encyclopedia of Material Science and Engineering*, Pergamon Press, (1986), p.841-88.
5. *Kirk-Othmer Encyclopedia of Chemical Technology*, 3rd ed., Vol. 6, John Wiley & Sons, Inc., (1979), p. 819-862
6. J. C. Bailar, H. J. Emeleus, R. Nyholm, A. F. Trotman-Dickerson, *Comprehensive Inorganic Chemistry*, Vol. 3, Pergamon Press, (1973), p.1-49.
7. V. L. Snoeyink, D. Jenkins, *Water Chemistry*, John Wiley & Sons, Inc., (1980), p. 36-59.
8. D. A. Jones, *Principles and Prevention of Corrosion*, Macmillan Publishing Co, (1996), p. 55-65, 79-101, 115-139.
9. U. R. Evans, *Corrosion and Corrosion Control, An Introduction to Metallic Corrosion*, 3rd ed., John Wiley & Sons, Inc., (1985), p.60-89, 327-340.
10. B. D. Craig, *Fundamental Aspects of Corrosion Films in Corrosion Science*, Plenum Press (1991), p. 9-37.
11. L. L. Shreir, *Corrosion, Metal/Environment Reactions*, John Wiley & Sons, Inc., Vol. 1 (1963), p.27-59.
12. J. C. Scully, *The Fundamentals of Corrosion*, 3rd ed., UK, Pergamon Press, (1990), p.107-120.
13. P. V Shigoev, *Electrolytic and Chemical Polishing*, Freund, (1974), p.9-29, 60-89, 111-114.

14. W. Y. Hsu, Q. Z. Hong, et al., Trench fill with low pressure long throw sputtering and the microstructure of damascene-fabricated Cu interconnects, *Advanced Metallization and Interconnect Systems for ULSI Applications in 1997*. (Materials Research Society Conference Proceedings, Vol. 514.) Materials Research Society (1998), p. 413-419.
15. K. K. Wong, S. Kaja, P. W. Dehaven, Metallization by Plating for High Performance Multichip Modules, *IBM Journal of Research and Development*, Vol. 42, No. 5, (1998).
16. J. Farkas, et al, Technology challenges for soft metal CMP in inlaid metallization, *Advanced Metallization and Interconnect Systems for ULSI Applications in 1997*. (Materials Research Society Conference Proceedings, Vol. 514.) Materials Research Society (1998), p.523-533.
17. R. J. Contolini, A. F. Bernhart, S. T. Mayer, Electrochemical Planarization for Multilevel Metallization, *Journal of the Electrochemical Society*, Vol. 1, No. 9, (1994), p.2503-2509.
18. J. Flis, *Corrosion of Metals and Hydrogen-Related Phenomena*, Polish Scientific Publishers, Warsaw, Poland, (1991), p. 152-157.
19. H. F. Walton, The Anode Layer in the Electrolytic Polishing of Copper, *Journal of the Electrochemical Society*, Vol. 97, (1950), p. 219-226.
20. R. Vidal, A. C. West, Copper Electropolishing in Concentrated Phosphoric Acid, *Journal of the Electrochemical Society*, Vol. 142, No. 8, (1995), p. 2682-2688.
21. K. Kojima, C. W. E. Tobias, Solution Side Transport Processes in Electropolishing of Copper in Phosphoric Acid, *Journal of the Electrochemical Society*, Vol. 120, No. 8, (1973), p. 1026-1033.
22. M. G. Foud, F. N. Zein, M. L. Ismail, A Study of Mass Transfer in Electropolishing of Copper, *Electrochemical Acta*, Vol. 16, (1971), p.1477-1487.
23. P. Neufeld, D. Southall, Gas Evolution and Pitting in Electropolishing, *Transaction of the Institute of Metal Finishing*, Vol. 54, Issue 1, (1976), p. 40-44.
24. P. Neufeld and T. Zervas, The Relationship Between Polarization Characteristics and the Electropolishing Behavior of Copper, *Surface Technology*, (1979), p. 129-135.
25. J. L. Fang., N. J. Wu, Determination of Composition of Viscous Liquid Film on Electropolishing Copper Surface by XPS and AES, *Journal of the Electrochemical Society*, Vol. 136, (December, 1989), p. 3800-3803.